RSC Advances

PAPER

Cite this: *RSC Adv.*, 2016, **6**, 107556

Synthesis of 2-arylated thiadiazolopyrimidones by Suzuki–Miyaura cross-coupling: a new class of nucleotide pyrophosphatase (NPPs) inhibitors†

Behzad Jafari,[a] Nazym Yelibayeva,[ab] Meirambek Ospanov,[ab] Syeda Abida Ejaz,[c] Saira Afzal,[c] Shafi Ullah Khan,[c] Zharylkasyn A. Abilov,[b] Mirgul Z. Turmukhanova,[b] Sergey N. Kalugin,[b] Sayfidin Safarov,[d] Joanna Lecka,[ef] Jean Sévigny,[ef] Qamar Rahman,[ag] Peter Ehlers,[ah] Jamshed Iqbal[c] and Peter Langer*[ah]

Over expression of nucleotide pyrophosphatase (NPPs) activity is associated with chondrocalcinosis, osteoarthritis, type 2 diabetes, neurodegenerative diseases, allergies and cancer metastasis. The potential of NPPs inhibitors as therapeutic agents, and the scarceness of their structure–activity relationship, encouraged us to develop new NPP inhibitors. Specifically, 2-bromo-7-methyl-5-oxo-5*H*-1,3,4-thiadiazolopyrimidine and its corresponding 6-fluoro derivatives were synthesized *via* a Suzuki–Miyaura reaction. The cross-coupling reaction with different arylboronic acids gave desired coupling products in good to excellent yields and showed wide functional group tolerance. Furthermore, all compounds were investigated for their potential to inhibit two families of ecto-nucleotidases, *i.e.* nucleoside triphosphate diphosphohydrolases (NTPDase) and NPPs. Interestingly, our compounds were identified as selective inhibitors of NPPs. Among derivatives **5a–5i**, compound **5i** ($IC_{50} \pm SEM = 0.39 \pm 0.01$ μM) was found to be the most potent inhibitor of h-NPP1 and compound **5h** ($IC_{50} \pm SEM = 1.02 \pm 0.05$ μM) was found to be the most potent inhibitor of h-NPP3. Similarly, for fluorinated thiadiazolopyrimidones, derivative **6e** ($IC_{50} \pm SEM = 0.31 \pm 0.01$ μM) exhibited the best inhibition of NPP1 and it was found that this compound exhibited ≈28 fold improvement in inhibitory potential as compared with the reference control *i.e.* Suramin ($IC_{50} \pm SEM = 8.67 \pm 1.3$ μM). Moreover, homology modelling and molecular docking studies of both inhibitors were carried out to suggest the putative binding mode of inhibitors with the respective enzyme *i.e.* h-NPP1 and h-NPP3.

Received 12th September 2016
Accepted 28th October 2016

DOI: 10.1039/c6ra22750c

www.rsc.org/advances

Introduction

Extracellular nucleotides and nucleosides are an important class of signaling molecules that are present in both the peripheral nervous system (PNS) and the central nervous system (CNS).[1] Generally, nucleotides are released from the cells or by selective transport through the plasma membrane. But nucleotides can also be generated extracellularly by adenylate kinases and nucleoside diphosphokinases.[2] Extracellular nucleotides exert their effects through two major receptor subfamilies P2X and P2Y. P2X receptors are ligand gated ion channels which consist of a family of seven receptors and mainly bind ATP. They are responsible for a large variety of responses including fast transmission at central synapses, macrophage activation, contraction of smooth muscle cells, platelet aggregation and apoptosis.[3,4] Moreover these receptors also play a role in neurodegeneration, inflammation and cancer. On the other hand, P2Y receptors are a group of eight G-protein coupled receptors, which mainly bind both purine and pyrimidine nucleotides and are associated with cell cytotoxicity, differentiation, migration and cell proliferation mechanisms.[5]

Considering their significance in intracellular signaling, the extracellular level of nucleotides is tightly maintained by a variety of cell surface located enzymes named ecto-nucleotidases.[6] In this regard, nucleoside triphosphate

[a]*Institut für Chemie, Universität Rostock, Albert-Einstein-Str. 3a, 18059 Rostock, Germany. E-mail: peter.langer@uni-rostock.de; Fax: +49 381 4986412; Tel: +49 381 4986410*

[b]*Al-Farabi Kazakh National University, Al-Farabi ave. 71, 050040 Almaty, Kazakhstan*

[c]*Centre for Advanced Drug Research, COMSATS Institute of Information Technology, Abbottabad, Pakistan*

[d]*Institute of Chemistry, Tajikistan Academy of Sciences, ul. Aini 299, Dushanbe, 734063 Tajikistan*

[e]*Département de microbiologie-infectiologie et d'immunologie, Faculté de Médecine, Université Laval, Québec, QC, G1V 0A6, Canada*

[f]*Centre de Recherche du CHU de Québec – Université Laval, Québec, QC, G1V 4G2, Canada*

[g]*Amity University, Lucknow Campus, Viraj Khand-5, Gomti Nagar, Lucknow-226010, India*

[h]*Leibniz Institut für Katalyse an der Universität Rostock e.V. (LIKAT), Albert-Einstein-Str. 29a, 18059 Rostock, Germany*

† Electronic supplementary information (ESI) available. See DOI: 10.1039/c6ra22750c

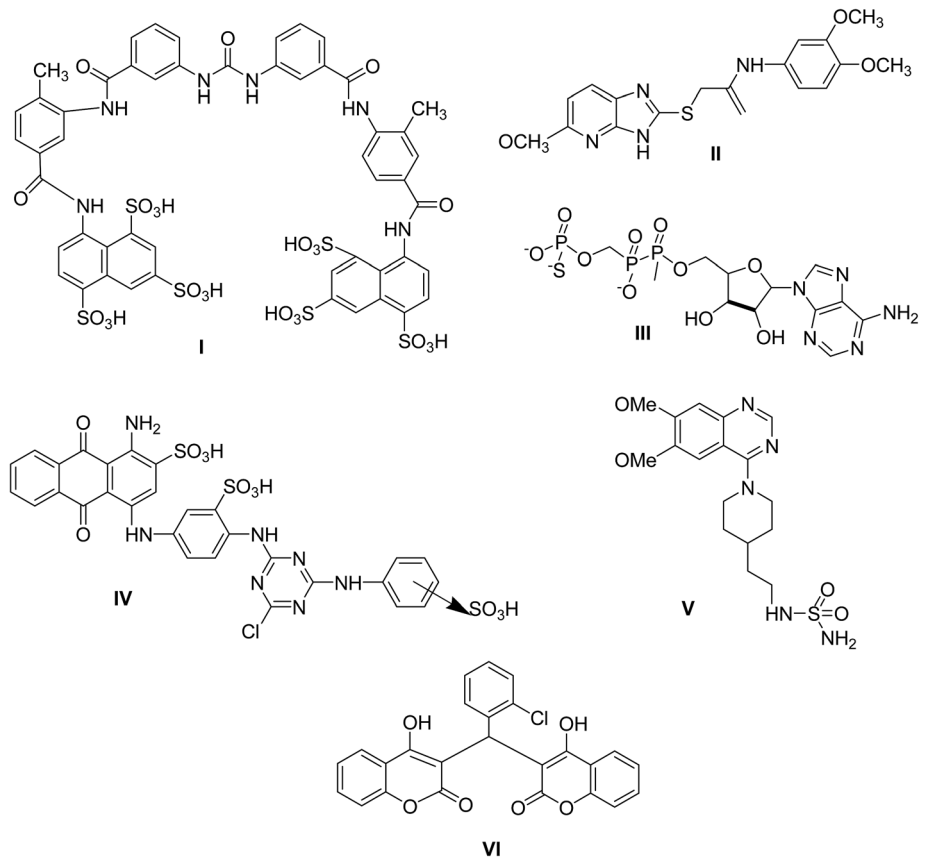

Fig. 1 Known inhibitors of NPP1. Suramin (I),[20b] thioacetamide derivative (II),[20c] ATP analogue (III),[20c] reactive blue (IV),[20b] quinazoline-4-piperidine-4-ethylsulfamide derivative (V)[20d] and biscoumarine derivative (VI).[20c]

diphosphohydrolases (NTPDase) and nucleotide pyrophosphatase (NPPs) are of particular interest which regulate the nucleotide signaling by controlling the rate, timing and amount of nucleotide degradation.[7,8] NTPDases represent a large family of ectonucleotidases which include eight members designated as NTPDase1–8. They dephosphorylate a variety of nucleoside triphosphates (*e.g.* ATP and UTP) and diphosphates (*e.g.*, ADP and UDP) with different abilities and exclusively in the presence of divalent cations (Ca^{2+} or Mg^{2+}).[9a] Each NTPDase member possesses different enzymatic properties and a separate cellular expression. They are responsible for the regulation of a multiplicity of biological processes, such as neurotransmission, cardiac function, liver glycogen metabolism and inflammation.[9b] Four members of this family, namely NTPDase1, NTPDase2, NTPDase3 and NTPDase8, are located at the surface of the plasma membrane and are responsible for controlling nucleotide signalling by activating P2 receptors. NTPDase1 hydrolyzes ATP and ADP equally. In contrast, NTPDase2 is a preferential triphosphonucleosidase, whereas NTPDase3 and NTPDase8 are functional intermediates between NTPDase1 and 2.[10,11]

Another member of the same family, nucleotide pyrophoshatases (NPPs), are also involved in the hydrolysis of nucleotides. This family consists of seven closely related members that are numbered according to their order of discovery.[12,13] They are widely distributed in tissues and exist either as transmembrane proteins or as secreted proteins in the extracellular space. To date, only three members, *i.e.* NPP1, NPP2 and NPP3, have been studied in detail.[14] These members possess a wide range of substrate specificities and are responsible for hydrolyzing the pyrophosphate and phosphodiester bonds in a variety of compounds.[15] For instance, NPP1 and NPP 3 catalyze the hydrolysis of nucleoside tri/di phosphate, oligonucleotides, diadenosine polyphosphate, flavin adenine dinucleotide, nicotinamide adenine dinucleotide (NAD^+), and uracil diphosphate (UDP) sugars.[16] As these enzymes play an important role in maintaining a balanced level of nucleotides, they are of critical importance in nucleotide recycling, stimulation of cell motility, regulation of extracellular pyrophosphate levels and modulation of purinergic receptor signaling. In addition, they are also proposed to be involved in the regulation of insulin receptors and activity of ectokinases.[17]

The presence of NPP1 has been described in various tissues, where its over expression can lead to many disorders, such as chondrocalcinosis or hypophosphatasia.[18] Likewise, various other diseases, such as angiogenesis, type 2 diabetes, neurodegenerative disorders, bone mineralization dysfunction, cell motility and migration and tumor cell invasion have been associated with abnormal expression of NPPs.[19] Numerous studies have established the importance of NPPs as potential

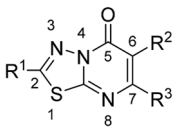

Fig. 2 2,6,7-Trisubstituted-5*H*-[1,3,4]-thiadiazolo[3,2-*a*]pyrimidin-5-one.

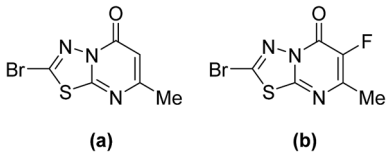

Fig. 3 2-Bromothiadiazolopyrimidones used in this study.

targets for the treatment of various diseases including hypophosphatasia, chondrocalcinosis, and insulin resistance. Similarly, inhibitors of NPP3 may also find useful application in the treatment of neurodegenerative diseases and allergies as well as in the prevention of cancer metastasis.[20a] To date, many inhibitors of NPPs have been identified, but they often exhibit a non-selective behaviour on other ectonucleotidases. Therefore, there is a need to explore potent and selective inhibitors of NPPs that would be helpful in treating various relevant pathological conditions.

We have chosen thiadiazolopyrimidones as scaffold for our studies as this type of heterocyclic core structure represents an important scaffold in pharmaceutical research and shows a huge variety of biological activities which include activity against cancer,[21] platelet aggregation,[22] xanthine oxidase activity for the treatment of gout[23] as well as activity for the medication of diseases related to central nervous system.[24] Furthermore, related compounds are reported as antimicrobial, antibacterial, anti-allergic activity or anti-inflammatory agents.[25] From the synthetic viewpoint we felt that the use of transition metal catalysed coupling reactions would greatly improve the accessibility of new derivatives of thiadiazolopyrimidones from a common starting material without the need of tedious syntheses of the starting materials. Based on the pharmacological activity know (see above) and based on initial docking studies we expected that arylated thiadiazolopyrimidones might be promising nucleotide pyrophosphatase (NPPs) inhibitors. The carbonyl group and nitrogen atoms in the heterocyclic core structure are ideally located to interact with the enzyme. An additional important point was the accessibility of both a fluorinated and non-fluorinated series based on our synthetic experience with this type of molecule. Fluorine present in heterocyclic core structures can have an important impact on the biological activity, because of the metabolic stability of the C–F bond and because of a change of the electronic situation combined with increased lipophilicity. Therefore, the thiadiazolopyrimidone core structure allowed us to investigate fluorinated and non-fluorinated core structures, besides the presence of fluorine in selected arylboronic acids used by us as mentioned above (Fig. 1).

Thiadiazolopyrimidones are easily available by simple condensation reactions of commercially available 2-aminothiadiazole with corresponding β-ketoesters in an acidic reaction medium.[26] Thus, functionalisation of positions 5 and 6 of thiadiazolopyrimidones is easily achieved by the choice of the appropriate β-ketoester. However, a functionalisation of position 2 is more complicated and requires corresponding aminothiadiazoles which have to be tediously synthesized (Fig. 2).[27]

Recently, the groups of Shukurov and Kukaniev synthesized 2-bromothiadiazolopyrimidones by simple bromination of aminothiadiazole and subsequent condensation with several β-ketoesters.[28] Products were applied in S_NAr reactions using N- and S-nucleophiles as well as CH-acidic carbonyl compounds. We decided to investigate the functionalisation of 2-bromothiadiazolopyrimidones by the Suzuki–Miyaura cross-coupling protocol. This building-block strategy will give access to a broad variety of 2-arylated thiadiazolopyrimidones. For our study we chose 7-methyl-2-bromo-5*H*-[1,3,4]-thiadiazolo[3,2-*a*]pyrimidin-5-one (a) as well as 2-bromo-6-fluoro-7-methyl-[1,3,4]-thiadiazolo[3,2-*a*]pyrimidin-5-one (b), because of the importance of fluorine in biological active compounds, as model substrates (Fig. 3). A great variety of aryl substituents were successfully introduced. We have selected the aryl substituents based on their electronic and steric aspects and 17 sterically and electronically different groups were used. In addition, we varied the position of the substituents at the phenyl group. A variety of alkyl, aryl and oxygen containing substituents were used. In addition, electron withdrawing substituents, such as nitro and cyano, were successfully employed. Due to the considerable pharmacological importance of fluorinated aryl groups, we also used three different fluorinated substituents. We then investigated these derivatives as potential inhibitors of nucleotide pyrophosphatase/phosphodiesterase-1 (h-NPP1) and h-NPP3. The effects of these molecules were also tested on four other human ectonucleotidases, nucleoside triphosphate diphosphohydrolases (NTPDase) *i.e.* h-NTPDase1, h-NTPDase2, h-NTPDase3 and h-NTPDase8.

Results and discussion

At first we synthesised 2-bromo-thiadiazole **2** by simple bromination using commercially available 2-aminothiadiazole **1** and elemental bromine in acetic acid. Afterwards, 2-bromothiadiazolopyrimidones **4a** and **4b** were synthesized by condensation of **2** with appropriate β-ketoester **3a** and **3b** (Scheme 1).

With brominated thiadiazolopyrimidones **4a** and **4b** in hand, we started to test the arylation by the Suzuki–Miyaura reaction. As a first trial we used compound **4a** as the starting material and adapted conditions from Copin *et al.*, who synthesised arylated imidazothiadiazoles using $Pd(OAc)_2$ in the presence of bidentate xantphos ligand, but using conventional heating instead of a microwave reactor.[29] Moreover, we used *o*-tolylboronic acid as a nucleophile. Using these conditions, we isolated the desired product **5a** in excellent 88% yield. Thus, no further optimization of the reaction condition was required and

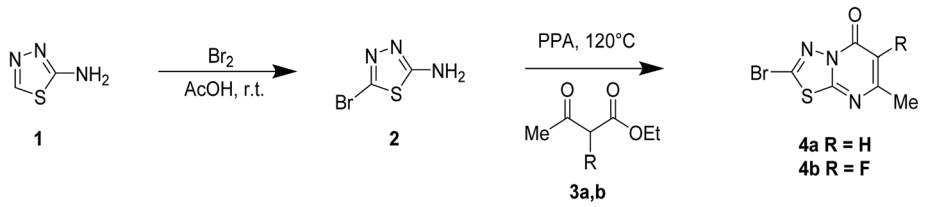

Scheme 1 Synthesis of starting materials **4a** and **4b**.[28]

we started to test the scope of the reaction condition with **4a** (Table 1).

All compounds were isolated in very good yields using *ortho*-, *meta*- or *para*-substituted arylboronic acids. Using *para*-chlorophenylboronic acid led to slightly diminished 65% yields, which might be a result of a cross-coupling reaction at the carbon–chlorine bond as a side-reaction.

Next we evaluated starting material **3b** in this reaction. This fluorinated starting material worked well in the cross-coupling reaction and delivered corresponding products in very good yields ranging from 50–92% yield. Electron-rich and electron-poor arylboronic acids gave good isolated yields (Table 2). 4-Trifluoromethoxyphenylboronic acid **4p** resulted in reduced yields what is due to problems during the purification process by column chromatography. However, comparing starting materials **3a** and **3b**, **3b** gave slightly improved yields of cross-coupling products which might be explained by the electron-withdrawing nature of the fluorine substituent and according activation of the aryl halide.

Structure–activity relationship

Suramin is a well-known polyanionic compound that binds to almost all ecto-nucleotidases, but inhibited both NTPDases and NPPs non-selectively. It inhibited h-NTPDase1, 2, 3 & 8 with inhibitory value of 16.1 ± 1.02, 24.1 ± 3.01, 4.31 ± 0.41 & >100 μM, respectively, while it inhibited h-NPP1 & 3 with inhibitory value of 8.67 ± 1.3 and 1.27 ± 0.08 μM, respectively. Our newly synthesized derivatives of 2-bromo-7-methyl-5*H*-[1,3,4]thiadiazolo[3,2-*a*]pyrimidin-5-one (**4a**) *i.e.* **5a–5i**, and 2-bromo-6-fluoro-7-methyl-5*H*-[1,3,4]thiadiazolo[3,2-*a*]pyrimidin-5-one (**4b**) *i.e.* **6a–6q** were evaluated for their inhibitory potential on h-NTPDases and h-NPPs. It was found that these compounds, in comparison to NTPDases, were identified as selective inhibitors of NPPs even at lower concentrations *i.e.* 100 μM. These compounds exhibited low inhibitory response *i.e.* below 50% on four isozymes of h-NTPDase. Except **5a**, all the derivatives of either **4a** or **4b** exhibited dual inhibition of both isozymes of NPPs but exhibited more selective inhibition of h-NPP1.

The detailed structure–activity relationship of arylated products derived from 2-bromo-7-methyl-5*H*-[1,3,4]thiadiazolo[3,2-*a*]pyrimidin-5-one (**4a**) suggested that the introduction of 4-chlorophenyl substituent at position 2 of **4a** led to a potent inhibitor **5i**. This compound (**5i**) was found to be the most potent inhibitor of h-NPP1 (IC_{50} ± SEM = 0.39 ± 0.01 μM) exhibiting ≈23 fold more inhibition than the reference control used *i.e.* Suramin (IC_{50} ± SEM = 8.67 ± 1.3 μM). It can be suggested that the more inhibitory potential of this compound might be due to the presence of less reactive substituent, *i.e.* 4-chlorophenyl at position 2 of **4a** which make the ring stable. This was further justified by comparing the activity of this compound with the other derivatives having more reactive substituent. For example, introduction of methyl group at *o*, *m*- or *p*-position (**5g**, **5h** & **5a**) resulted in reduced activity, in comparison to **5i**. In this case, dimethyl substitution (**5g** & **5h**) showed better improvement in inhibitory potential as compared to the mono-substituted methyl (**5a**). Interestingly, dimethyl substitution at *m*-position exhibited high inhibitory potential *i.e.* IC_{50} ± SEM = 0.41 ± 0.01 μM, however, the activity was only moderately reduced when one *m*-methyl group was shifted to *p*-position of phenyl ring (**5h**) *i.e.* IC_{50} ± SEM = 0.43 ± 0.02 μM. This shifting of methyl group from *m*- to *p*-position was appeared to be essential for h-NPP3 activity. Likewise, the replacement of the di-substituted methyl group by mono-substituted methyl group from *m*–*p* to *o*-position (**5a**) reduced or nearly abolished the activity against h-NPP1 but exhibited improved inhibitory potential against h-NPP3 with IC_{50} value of 2.19 ± 0.22 μM. Interestingly, the potency against h-NPP1 was greatly reduced when the 4-chlorophenyl was replaced by 4-ethoxyphenyl as in **5e** or 4-methoxyphenyl as in **5d** or ethylated phenyl as in **5c** (Table 2). The reason behind this effect might be due to the presence of ethoxy and methoxy groups which are electron donating, less reactive than methyl and are moderately activating the benzene ring. As a result of this, it increases electronic cloud, produces more stearic hindrance, less reactivity of the compound and ultimately exhibited less inhibitory potential.

The set of fluorinated 5*H*-[1,3,4]thiadiazolo[3,2-*a*]pyrimidin-5-ones derived from **4b**, *i.e.* **6a–6q** exhibited more significant inhibitory results as compared to products derived from non-fluorinated educt **4a**. The obtained results suggested that the presence of fluorine at 6-position of the ring is responsible for the improvement in inhibitory values. As presence of electronegative fluorine increases the electron density on thiadiazolopyrimidine ring, thus the substitution of less reactive group at phenyl ring attached at position 2 resulted in the improvement of inhibitory values towards both isozymes. An interesting behavior was observed in case of 4-chlorophenyl substitution *i.e.* derivative **6l**. It exhibited less inhibition of h-NPP1 as compared to **5i** due to the presence of two electronegative atoms *i.e.* F and Cl which decreases the electron density on the functional ring *i.e.* thiadiazolopyrimidine and make the ring unstable. It was observed that introduction of more reactive methyl as 3,5-dimethylphenyl at position 2 of **4b**, led to the potent inhibitor **6e**. This compound was found to be the most

Table 1 Synthesis of compounds 5a–5i [a]

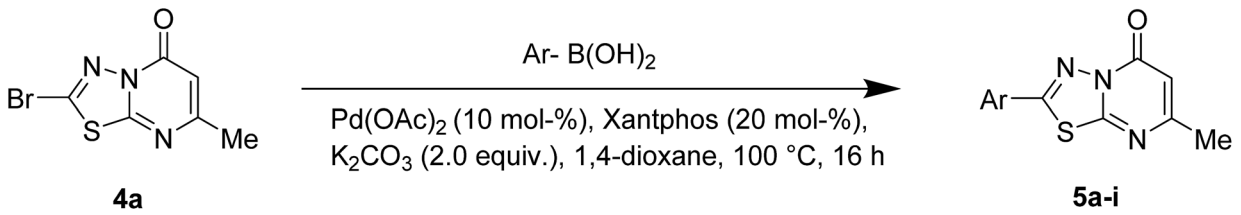

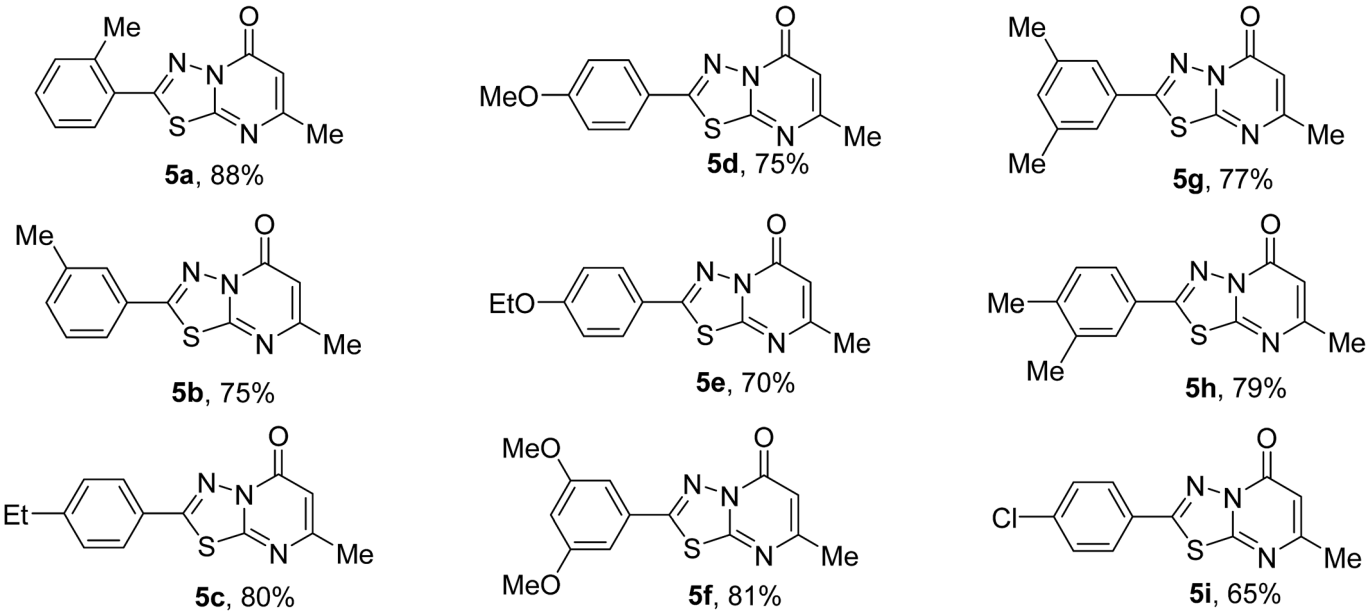

[a] Yield of isolated products.

potent inhibitor of h-NPP1 with the inhibitory value of 0.31 ± 0.01 μM, exhibiting maximum inhibition of h-NPP1 and it was found that this compound exhibited ≈28 fold improvement in inhibitory potential than the used reference control *i.e.* Suramin (IC_{50} ± SEM = 8.67 ± 1.3 μM). The shifting of one methyl group from *m*-position to *p*-position (**6d**) or introduction of single methyl group in the *p*-position (**6a**) led to a decrease in the activity of >4-fold as compared to **6e**. The introduction of *m*-substituted phenyl ring with electron withdrawing nitrogroup *i.e.* 3-nitrophenyl (**6f**), dramatically decreased the inhibitory activity against both h-NPPs. The effect was observed because of presence of nitro group at *m*-position of the ring, where it strongly deactivated the phenyl ring.

Likewise, the introduction of *m*- or *p*-substituted phenyl ring with electron donating methoxy group exhibited interesting behavior. For example: *p*-substituted phenyl ring, *i.e.* in case of 3-methoxyphenyl **6i**, led to 4 fold improved inhibition of h-NPP1 as compared to h-NPP3. Reverse effect was observed when phenyl ring was di-substituted at *m*-position, *i.e.* 3,5-dimethoxyphenyl in case of **6j** resulted in reduced inhibition of h-NPP1 but 2 fold improved inhibitory value against h-NPP3. The introduction of a halogen (chlorine or fluorine) substituent in the *p*- and *m*-position (**6l** & **6m**) exhibited atmost equipotent inhibitory activity against both h-NPPs *i.e.* h-NPP31 & 3.

It can be concluded from the obtained results that in case of **4a** derivatives, substitution of electron withdrawing group *i.e.* Cl resulted in improved inhibitory potential towards h-NPP1. While in case of **4b** derivatives, substitution with electronegative atom resulted in decreased inhibition of h-NPP1. Moreover, disubstitution of phenyl ring with electron donating groups at *m*-position, in both **4a** and **4b** derivatives, justifying the improved inhibition toward both isozymes (Table 3).

Mechanism of inhibition. Detailed kinetics studies were carried out for compound **6e** and **6j**, the most potent inhibitor of h-NPP1 and h-NPP3, respectively. The Lineweaver–Burk plot of both compounds visualizes the competitive mechanism of inhibition by showing the same *y*-intercept for uninhibited and inhibited enzyme (Fig. 4 and 5).

Homology modelling of human NPP1 and NPP3

Homology modelling is the most reliable and extensively used method for prediction of 3D structure of a protein in the absence of X-ray/NMR structures of target proteins.[30] X-ray crystallographic structures of h-NPP1 and h-NPP3 are not available in protein data bank. For this purposed homology modelling approach was used to predict the 3D model of targets, h-NPP1 and h-NPP3 enzymes. X-ray crystallographic

Table 2 Synthesis of products **6a–6q** [a]

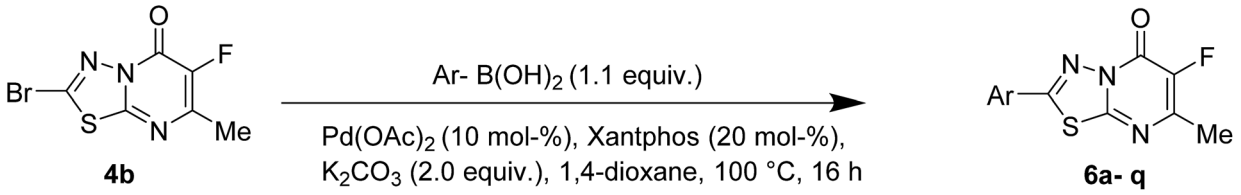

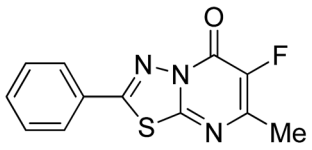
6a, 92%

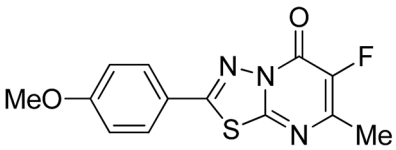
6g, 88%

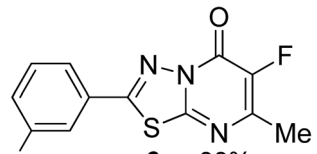
6m, 88%

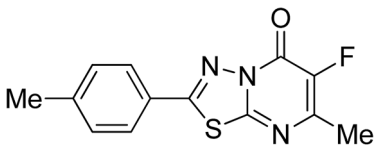
6b, 80%

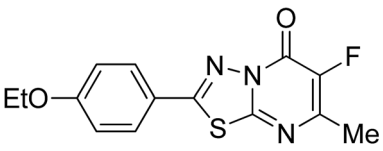
6h, 75%

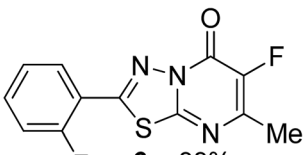
6n, 88%

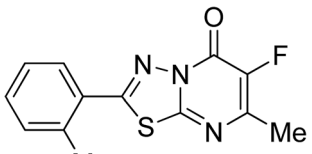
6c, 72%

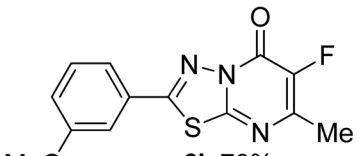
6i, 70%

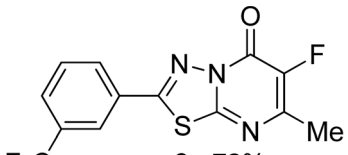
6o,72%

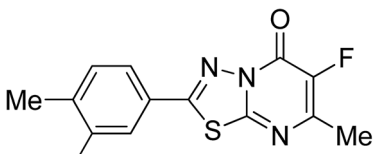
6d, 92%

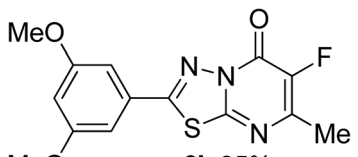
6j, 85%

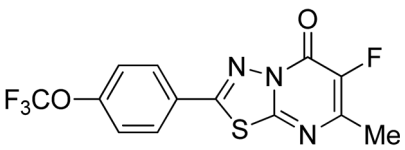
6p, 50%

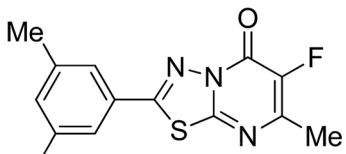
6e, 85%

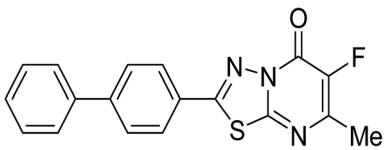
6k, 62%

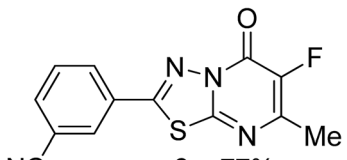
6q, 77%

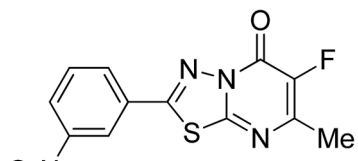
6f, 84%

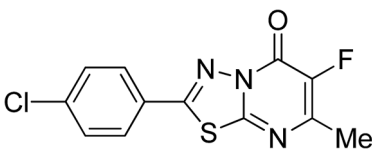
6l, 72%

[a] Yields of isolated product.

structure of mouse ectonucleotide pyrophosphatase-phosphodiesterase-1 (m-ENPP1, PDB ID 4B56) was used as template model to generate the homology model of target proteins. Homology modelling of target proteins were performed as that of previously reported method,[31] *via* Molecular Operating Environment (MOE 2104.0901).[32] Modelled structures of both targets *i.e.* h-NPP1 and h-NPP3 exhibited 80% and 52% sequence identity with template m-NPP1, respectively. Sequence and structural alignment of modelled proteins with template protein were also performed using superimpose and align utilities of MOE 2104.0901 (depicted in ESI†). Energy minimization, protonation and tautomer state of the amino acids were fixed using in-built utilities of MOE package such as Amber12:EHT and Protonate 3D.[33,34] RMSD between h-NPP1 modelled protein and m-NPP1 template protein was 0.613 Å over 816 residues while RMSD between h-NPP3 modelled protein and m-NPP1 template protein was 1.349 Å over 811 residues. The

Table 3 Nucleoside triphosphate diphosphohydrolase (h-NTPDase1, -2, -3 & -8) nucleotide pyrophosphatase (h-NPP1 & -3) inhibition data for the synthesized compounds[a]

		$IC_{50} \pm SEM$ (μM)					
Sr. no.	Codes	h-NTPDase1	h-NTPDase2	h-NTPDase3	h-NTPDase8	h-NPP1	h-NPP3
1	**5a**	—	—	—	—	—	2.19 ± 0.22
2	**5c**	—	—	—	—	2.26 ± 0.13	15.1 ± 1.89
3	**5d**	—	—	—	—	1.39 ± 0.13	7.37 ± 0.96
4	**5e**	—	—	—	—	0.69 ± 0.02	10.3 ± 1.09
5	**5g**	—	—	—	—	0.41 ± 0.01	6.28 ± 0.79
6	**5h**	—	—	—	—	0.43 ± 0.02	1.02 ± 0.05
7	**5i**	—	—	—	—	0.39 ± 0.01	4.18 ± 0.41
8	**6a**	—	—	—	—	0.83 ± 0.04	2.79 ± 0.31
9	**6b**	—	—	—	—	1.31 ± 0.05	2.01 ± 0.16
10	**6c**	—	—	—	—	0.85 ± 0.02	15.5 ± 1.56
11	**6d**	—	—	—	—	1.56 ± 0.16	2.89 ± 0.15
12	**6e**	—	—	—	—	0.31 ± 0.01	4.63 ± 0.62
13	**6f**	—	—	—	—	0.63 ± 0.03	4.39 ± 0.61
14	**6g**	—	—	—	—	1.24 ± 0.02	4.57 ± 0.86
15	**6i**	—	—	—	—	0.79 ± 0.02	2.87 ± 0.78
16	**6j**	—	—	—	—	2.01 ± 0.16	0.92 ± 0.02
17	**6k**	—	—	—	—	1.04 ± 0.14	2.21 ± 0.13
18	**6l**	—	—	—	—	1.11 ± 0.11	1.79 ± 0.03
19	**6m**	—	—	—	—	0.94 ± 0.07	0.94 ± 0.05
20	**6n**	—	—	—	—	0.37 ± 0.02	8.95 ± 1.08
21	**6o**	—	—	—	—	1.32 ± 0.32	4.67 ± 0.56
22	**6p**	—	—	—	—	0.39 ± 0.03	5.34 ± 0.71
23	**6q**	—	—	—	—	1.02 ± 0.11	12.2 ± 1.34
Positive control	**Suramin**	**16.1 ± 1.02**	**24.1 ± 3.01**	**4.31 ± 0.41**	**>100**	**8.67 ± 1.3**	**1.27 ± 0.08**

[a] Values are expressed as mean ± SEM of $n = 3$. The IC_{50} is the concentration at which 50% of the enzyme activity is inhibited.

generated homology modelled structures revealed good stereochemical property as shown in Ramachandran plot (see ESI†).[33] Ramachandran plot of homology modelled h-NPP1 showed that about 98.9% amino acid residue were fall in core and allowed region while in case of Ramachandran plot of homology modelled of h-NPP3 displayed that about 97.8% amino acid residues fall in core and allowed region (see ESI†).

Molecular docking

Molecular docking was carried out to investigate the putative binding interactions of most potent inhibitor inside the active site of respective target h-NPP1 and h-NPP3.[31] Fig. 6 showed binding interactions of compound **6e** in modelled h-NPP1 while Fig. 7 illustrated the binding interaction of compound **6j** inside the active site of modelled h-NPP3. Potent inhibitor of both modelled targets displayed a very correlative mode of

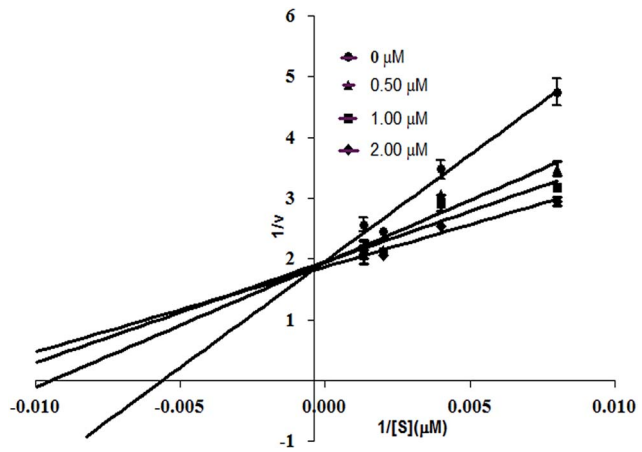

Fig. 4 Lineweaver–Burk plot of h-NPP1 inhibition by compound **6e**. *S*, concentration of substrate *p*-Nph-5-TMP (μM); concentration of **6e**: black circle, 0 μM; black triangle, 0.5 μM; black square, 1 μM; and black diamond, 2 μM.

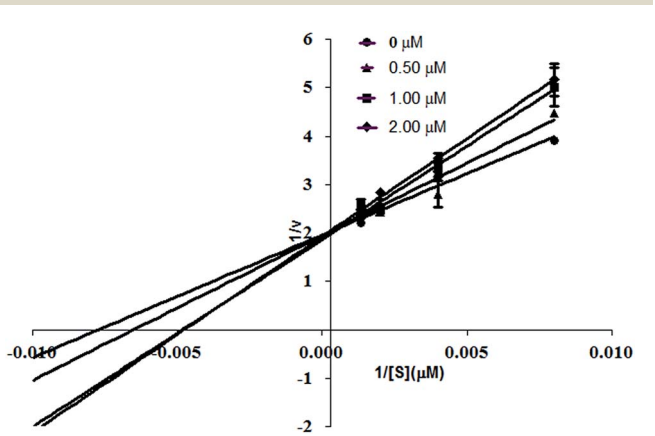

Fig. 5 Lineweaver–Burk plot of h-NPP3 inhibition by compound **6j**. *S*, concentration of substrate *p*-Nph-5-TMP (μM); concentration of **6j**: black circle, 0 μM; black triangle, 0.5 μM; black square, 1 μM; and black diamond, 2 μM.

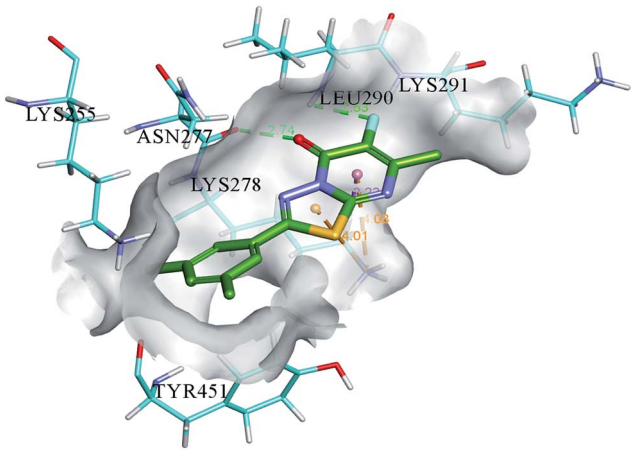

Fig. 6 Putative binding mode of **6e** (dark green colored) inside the active site of modelled h-NPP1 (cyan colored).

interaction with each other inside the active sites of modelled structure of target enzymes. Both potent compounds formed two hydrogen bonds (green dotted line) and two pi–cation interaction (gold dotted line) inside the active site of both modelled target, h-NPP1 and h-NNP3. Carbonyl oxygen of pyrimidine ring in both compounds formed one hydrogen bond with Asn277 in h-NPP1 and h-NP3 with a distance of 2.74 Å and 2.93 Å respectively. Substituted fluorine in pyrimidine ring in both potent compounds **6e** and **6j** also formed one hydrogen bond with Leu290 with a distance of 2.53 Å and 2.03 Å respectively. Pyrimidine and thiadiazole ring in both potent compounds also formed two pi–cation interactions with amino acid Lys278 with a distance of 4.01 Å and 3.95 Å inside the active site of both target enzymes.

Each methoxy side chain in **6j** compounds formed two additional hydrogen bonds in the active site of h-NPP3. In these two additional hydrogen bonds, one H-bond was formed between oxygen of one methoxy group and amino acid residue Lys255 with a distance of 1.99 Å while other H-bond was formed between oxygen of other methoxy group in compound **6j** and amino acid residue Tyr451 with a distance of 2.03 Å inside the active site of h-NPP3.

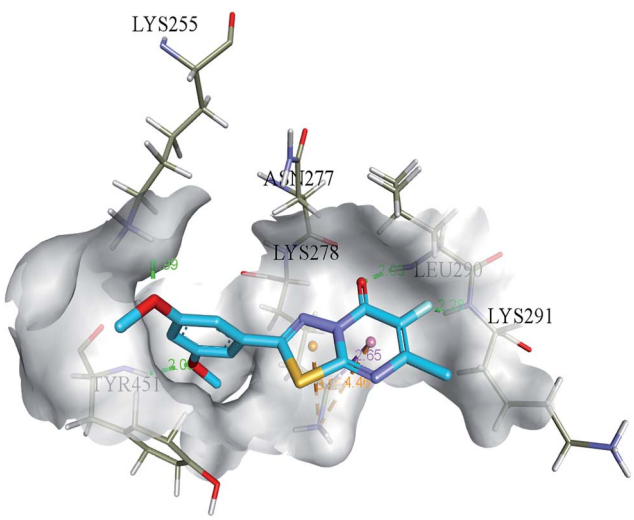

Fig. 7 Putative binding mode of **6j** (sky blue colored) inside the active site of modelled h-NPP3 (grey colored).

Conclusions

In conclusion, we developed a new building block strategy for the synthesis of 2-arylated thiadiazolopyrimidones using the Suzuki–Miyaura reaction. Our reaction conditions allows the facile synthesis of the products in generally good to very good yields what is represented by the application of two different thiadiazolopyrimidones. All the compounds were selective inhibitors of NPPs with little effect on h-NTPDase1, h-NTPDase2, h-NTPDase3 and h-NTPDase8. In addition, our data suggested that most of the compounds presented here inhibited h-NPP1 more efficiently than h-NPP3. Therefore these compounds appear as more selective inhibitors of h-NPP1. The results reported herein are of considerable interest for further applications in medicinal chemistry.

Experimental section

General procedure for the synthesis of 2-substituted-7-methyl-5*H*-1,3,4-thiadiazolo[3,2-*a*]pyrimidin-5-one and 2-substituted-6-fluoro-7-methyl-5*H*-1,3,4-thiadiazolo[3,2-*a*]pyrimidin-5-one

Mixture of 2-bromo-7-methyl-5*H*-1,3,4-thiadiazolo[3,2-*a*]pyrimidin-5-one (1.0 equiv., 0.407 mmol) or 2-bromo-6-fluoro-7-methyl-1,3,4-thiadiazolo[3,2-*a*]pyrimidin-5-one (1.0 equiv., 0.379 mmol), arylboronic acid (1.1 equiv.), palladium(II)acetate (0.1 equiv.), xantphos (0.2 equiv.), potassium carbonate (2.0 equiv.) was vigorously stirred and heated in dry 1,4-dioxane (2 mL) at 100 °C for 16 h. After cooling to room temperature, the reaction was diluted with water and extracted into ethyl acetate. The organic layer was dried with anhydrous sodium sulfate and the solvent was evaporated. The crude compound was purified by flash column chromatography on silica gel (ethyl acetate : heptane).

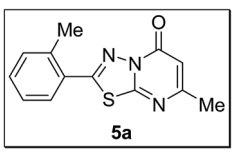

5a

7-Methyl-2-(2-methylphenyl)-5*H*-1,3,4-thiadiazolo[3,2-*a*]-pyrimidin-5-one (5a). According to the general procedure, using 2-methylphenylboronic acid afforded 100 mg of product **5a** (88%) as a yellow solid; mp (135–136 °C); ^{1}H NMR (250 MHz, $CHCl_3$) δ 7.60–7.63 (m, 1H, CH_{Ar}), 7.41–7.47 (m, 1H, CH_{Ar}), 7.28–7.36 (m, 2H, CH_{Ar}), 6.32 (d, ^{4}J = 0.60 Hz, 1H, $CH_{Het\text{-}Ar}$), 2.64 (s, 3H, CH_3), 2.38 (br, s, 3H, CH_3); ^{13}C NMR (62 MHz, $CDCl_3$) δ 163.40 (C_{Ar}), 161.34 (C_{Ar}), 158.78 (C_{Ar}), 157.09 (C_{Ar}), 137.99 (C_{Ar}), 132.07 (C_{Ar}), 131.94 (CH_{Ar}), 130.48 (CH_{Ar}), 127.54 (CH_{Ar}), 126.63 (CH_{Ar}), 107.73 ($CH_{Het\text{-}Ar}$), 23.96 (CH_3), 21.56 (CH_3); IR (ATR) ν 3054 (w), 2962 (w), 2921 (w), 1681 (s), 1576 (s), 1498 (s), 1440 (m), 1390 (m), 1364 (m), 1249 (m), 1033 (w), 964 (m), 825 (m), 766 (s), 696 (m), 609 (m) cm^{-1}; MS *m*/*z* 257 (M^+, 100),

229(10), 174(15), 149(32), 112(24), 91(21); HRMS calcd for $C_{13}H_{11}ON_3S$ 257.06173 found 257.06168; anal. calcd for $C_{13}H_{11}ON_3S$: C, 60.68; H, 4.31; N, 16.33; S, 12.46 found: C, 60.77; H, 4.44; N, 16.94; S, 12.08.

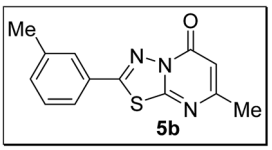

5b

7-Methyl-2-(3-methylphenyl)-5*H*-1,3,4-thiadiazolo[3,2-*a*]-pyrimidin-5-one (5b). According to the general procedure, using 3-methylphenylboronic acid afforded 85 mg of product **5b** (75%); yellow solid; mp (167–168 °C); ^{1}H NMR (300 MHz, $CHCl_3$) δ 7.83 (d, ^4J = 0.54 Hz, 1H, CH_{Ar}), 7.68–7.71 (m, 1H, CH_{Ar}), 7.38–7.40 (m, 2H, CH_{Ar}), 6.33 (d, ^4J = 0.56 Hz, 1H, $CH_{Het\text{-}Ar}$), 2.43 (s, 3H, CH_3), 2.39 (d, ^4J = 0.75 Hz, 3H, CH_3); ^{13}C NMR (62 MHz, $CDCl_3$) δ 163.36 (C_{Ar}), 161.09 (C_{Ar}), 159.19 (C_{Ar}), 157.21 (C_{Ar}), 139.66 (C_{Ar}), 133.93 (C_{Ar}), 129.38 (CH_{Ar}), 128.29 (CH_{Ar}), 128.18 (CH_{Ar}), 125.20 (CH_{Ar}), 107.86 ($CH_{Het\text{-}Ar}$), 23.95 (CH_3), 21.32 (CH_3); IR (ATR) ν 3485 (w), 3049 (w), 2955 (w), 2854 (w), 1689 (s), 1670 (m), 1502 (s), 1441 (w), 1393 (m), 1364 (m), 1175 (w), 1042 (w), 906 (w), 858 (w), 777 (m), 689 (m), 609 (w) cm^{-1}; MS *m*/*z* 257 (M^+, 100), 229(13), 135(25), 112(77), 91(16); HRMS calcd for $C_{13}H_{11}ON_3S$ 257.06173 found 257.06224; anal. calcd for $C_{13}H_{11}ON_3S$: C, 60.68; H, 4.31; N, 16.33; S, 12.46 found: C, 60.59; H, 4.51; N, 16.53; S, 12.15.

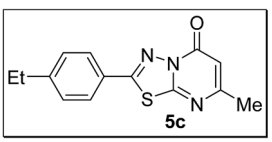

5c

7-Methyl-2-(4-ethylphenyl)-5*H*-1,3,4-thiadiazolo[3,2-*a*]pyrimidin-5-one (5c). According to the general procedure, using 4-ethylphenylboronic acid afforded 89 mg of product **5c** (80%); yellow solid; mp (165–166 °C); ^{1}H NMR (300 MHz, $CHCl_3$) δ 7.87 (d, ^3J = 8.37 Hz, 2H, CH_{Ar}), 7.34 (d, ^3J = 8.52 Hz, 2H, CH_{Ar}), 6.32 (d, ^4J = 0.75 Hz, 1H, $CH_{Het\text{-}Ar}$), 2.73 (q, ^3J = 7.55 Hz, 2H, CH_2), 2.39 (d, ^4J = 0.75 Hz, 3H, CH_3) 1.27 (t, ^3J = 7.55 Hz, 3H, CH_3); ^{13}C NMR (62 MHz, $CDCl_3$) δ 163.16 (C_{Ar}), 161.21 (C_{Ar}), 157.22 (C_{Ar}), 150.30 (C_{Ar}), 134.18 (C_{Ar}), 129.16 (C_{Ar}), 128.05 (CH_{Ar}), 125.95 (CH_{Ar}), 107.95 ($CH_{Het\text{-}Ar}$), 28.95 (CH_2), 23.94 (CH_3), 15.32 (CH_3); IR (ATR) ν 3079 (w), 3044 (w), 3008 (w), 2851 (w), 1921 (w), 1611 (m), 1515 (w), 1401 (s), 1342 (s), 1180 (s), 1021 (m), 819 (m), 731 (s), 681 (s), 638 (w), 528 (m) cm^{-1}; MS *m*/*z* 271 (M^+, 100), 243(13), 149(13), 134(34), 112(93), 85(14); HRMS calcd for $C_{14}H_{13}ON_3S$ 271.07738 found 271.07744; anal. calcd for $C_{14}H_{13}ON_3S$: C, 61.97; H, 4.83; N, 16.33; S, 11.83 found: C, 61.77; H, 4.44; N, 16.74; S, 12.08.

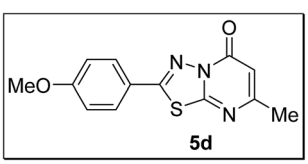

5d

7-Methyl-2-(4-methoxyphenyl)-5*H*-1,3,4-thiadiazolo[3,2-*a*]-pyrimidin-5-one (5d). According to the general procedure, using 4-methoxyphenylboronic acid afforded 84 mg of product **5d** (75%); yellow solid; mp (237–238 °C); ^{1}H NMR (250 MHz, $CDCl_3$) δ 8.89 (d, ^3J = 8.82 Hz, 2H, CH_{Ar}), 7.89 (d, ^3J = 8.82 Hz, 2H, CH_{Ar}), 6.31 (d, ^4J = 0.78 Hz, 1H, $CH_{Het\text{-}Ar}$), 3.88 (s, 3H, OMe), 2.39 (d, ^4J = 0.63 Hz, 3H, CH_3); ^{13}C NMR (62 MHz, $CDCl_3$) δ 163.58 (C_{Ar}), 162.57 (C_{Ar}), 161.08 (C_{Ar}), 158.83 (C_{Ar}), 156.96 (C_{Ar}), 129.68 (C_{Ar}), 120.73 (CH_{Ar}), 114.94 (CH_{Ar}), 107.82 ($CH_{Het\text{-}Ar}$), 55.78 (OMe), 23.66 (CH_3); IR (ATR) ν 3062 (w), 2961 (w), 2848 (w), 1684 (s), 1650 (w), 1601 (m), 1570 (m), 1490 (s), 1258 (s), 1174 (m), 1019 (m), 835 (m), 700 (m), 591 (m) cm^{-1}; MS *m*/*z* 273 (M^+, 100), 245(8), 151(41), 133(23), 112(81), 94(16); HRMS calcd for $C_{13}H_{11}O_2N_3S$ 273.05665 found 273.05669; anal. calcd for $C_{13}H_{11}O_2N_3S$: C, 57.13; H, 4.06; N, 15.37; S, 11.73 found: C, 57.51; H, 4.44; N, 15.74; S, 12.08.

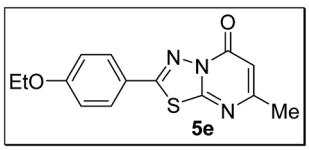

5e

7-Methyl-2-(4-ethoxyphenyl)-5*H*-1,3,4-thiadiazolo[3,2-*a*]-pyrimidin-5-one (5e). According to the general procedure, using 4-ethoxyphenylboronic acid afforded 79 mg of product **5e** (70%); brown solid; mp (151–152 °C); ^{1}H NMR (300 MHz, $CHCl_3$) δ 7.88 (d, ^3J = 8.98 Hz, 2H, CH_{Ar}), 6.98 (d, ^3J = 8.98 Hz, 2H, CH_{Ar}), 6.31 (d, ^4J = 0.78 Hz, 1H, $CH_{Het\text{-}Ar}$), 4.11 (q, ^3J = 7.00 Hz, 2H, OCH_2), 2.37 (d, ^4J = 0.63 Hz, 3H, CH_3), 1.45 (t, ^3J = 6.93 Hz, 3H, CH_3); ^{13}C NMR (62 MHz, $CDCl_3$) δ 163.16 (C_{Ar}), 163.09 (C_{Ar}), 161.22 (C_{Ar}), 158.68 (C_{Ar}), 157.20 (C_{Ar}), 129.66 (C_{Ar}), 120.65 (CH_{Ar}), 115.34 (CH_{Ar}), 107.84 ($CH_{Het\text{-}Ar}$), 64.13 (OCH_2), 23.90 (CH_3), 14.77 (CH_3); IR (ATR) ν 3050 (w), 2982 (w), 2936 (w), 2878 (w), 1702 (s), 1693 (s), 1605 (m), 1496 (s), 1384 (m), 1316 (w), 1305 (w), 1259 (s), 1172 (m), 1029 (m), 824 (m), 699 (m), 603 (m) cm^{-1}; MS *m*/*z* 287 (M^+, 100), 259(7), 149(11), 137(19), 112(62), 94(8); HRMS calcd for $C_{14}H_{13}O_2N_3S$ 287.07230 found 287.07210; anal. calcd for $C_{14}H_{13}O_2N_3S$: C, 58.52; H, 4.56; N, 14.64; S, 11.16 found: C, 58.51; H, 4.49; N, 15.04; S, 11.08.

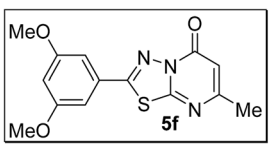

5f

7-Methyl-2-(2,6-dimethoxyphenyl)-5*H*-1,3,4-thiadiazolo[3,2-*a*]pyrimidin-5-one (5f). According to the general procedure, using 3,5-dimethoxyphenylboronic acid afforded 100 mg of product **5f** (81%); brown solid; mp (219–220 °C); ^{1}H NMR (300 MHz, $CHCl_3$) δ 7.84 (d, ^3J = 7.83 Hz, 2H, CH_{Ar}), 6.62 (t, ^3J = 2.25 Hz, 1H, CH_{Ar}), 6.32 (d, ^4J = 0.69 Hz, 1H, $CH_{Het\text{-}Ar}$), 3.85 (s, 6H, OCH_3), 2.38 (d, ^4J = 0.60 Hz, CH_3); ^{13}C NMR (62 MHz, $CDCl_3$) δ 163.51 (C_{Ar}), 161.47 (C_{Ar}), 161.02 (C_{Ar}), 158.93 (C_{Ar}), 157.21 (C_{Ar}), 143.53 (C_{Ar}), 130.06 (CH_{Ar}), 107.85 ($CH_{Het\text{-}Ar}$), 105.77 (CH_{Ar}), 55.95 (OMe), 23.98 (CH_3); IR (ATR) ν 3486 (m), 3449 (m), 3052 (w), 2953 (w), 1668 (s), 1564 (s), 1501 (s), 1362

(s), 1208 (m), 1182 (m), 1041 (s), 854 (m), 777 (m), 687 (m), 653 (m) cm^{-1}; MS *m*/*z* 303 (M^+, 100), 275(10), 181(17) 163(16), 140(5), 123 (10), 112(59); HRMS calcd for $C_{14}H_{13}O_3N_3S$ 303.06721 found 303.06710; anal. calcd for $C_{14}H_{13}O_3N_3S$: C, 55.43; H, 4.32; N, 13.85; S, 10.57 found: C, 56.01; H, 4.49; N, 13.34; S, 11.08.

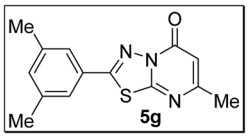

7-Methyl-2-(3,5-dimethylphenyl)-5*H*-1,3,4-thiadiazolo[3,2-*a*]-pyrimidin-5-one (5g). According to the general procedure, using 3,5-dimethylphenylboronic acid afforded 88 mg of product **5g** (79%); yellow solid; mp (216–217 °C); ^{1}H NMR (250 MHz, $CHCl_3$) δ 7.55 (s, 2H, CH_{Ar}), 7.19 (s, 1H, CH_{Ar}), 6.31 (s, 1H, $CH_{Het\text{-}Ar}$), 2.37 (s, 9H, CH_3); ^{13}C NMR (62 MHz, $CDCl_3$) δ 163.36 (C_{Ar}), 161.10 (C_{Ar}), 159.30 (C_{Ar}), 157.22 (C_{Ar}), 139.42 (C_{Ar}), 134.83 (C_{Ar}), 128.19 (CH_{Ar}), 125.55 (CH_{Ar}), 107.29 ($CH_{Het\text{-}Ar}$), 23.96 (CH_3), 21.19 (CH_3); IR (ATR) ν 3031 (w), 2946 (w), 2914 (w), 1690 (s), 1567 (s), 1492 (s), 1354 (w), 1198 (w), 854 (m), 687 (m) cm^{-1}; MS *m*/*z* 271 (M^+, 100), 243(12), 149(22), 133(11), 112(82), 103 (7); HRMS calcd for $C_{14}H_{13}ON_3S$ 271.07738 found 271.07750; anal. calcd for $C_{14}H_{13}ON_3S$: C, 61.92; H, 4.83; N, 15.49; S, 11.82 found: C, 61.77; H, 4.44; N, 15.70; S, 11.88.

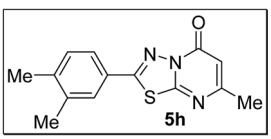

7-Methyl-2-(3,4-dimethylphenyl)-5*H*-1,3,4-thiadiazolo[3,2-*a*]-pyrimidin-5-one (5h). According to the general procedure, using 3,4-dimethylphenylboronic acid afforded 85 mg of product **5h** (77%); yellow solid; mp (175–176 °C); ^{1}H NMR (300 MHz, $CHCl_3$) δ 7.75 (d, ^3J = 1.38 Hz 1H, CH_{Ar}), 7.60 (dd, ^3J = 7.83 Hz, ^4J = 1.76 Hz, 1H, CH_{Ar}), 7.23 (d, ^3J = 7.83 Hz, 1H, CH_{Ar}), 6.30 (s, 1H, $CH_{Het\text{-}Ar}$), 2.36 (s, 9H, CH_3); ^{13}C NMR (62 MHz, $CDCl_3$) δ 163.31 (C_{Ar}), 161.10 (C_{Ar}), 159.17 (C_{Ar}), 157.24 (C_{Ar}), 142.75 (C_{Ar}), 138.21 (C_{Ar}), 130.62 (C_{Ar}), 128.54 (CH_{Ar}), 125.92 (CH_{Ar}), 125.47 (CH_{Ar}), 107.76 ($CH_{Het\text{-}Ar}$), 23.96 (CH_3), 20.13 (CH_3), 19.68 (CH_3); IR (ATR) ν 3562 (m), 3454 (m), 3043 (w), 2945 (w), 1685 (s), 1567 (s), 1488 (s), 1394 (m), 1263 (m), 1124 (m), 977 (m), 861 (m), 741 (m), 695 (m), 623 (m) cm^{-1}; MS *m*/*z* 271 (M^+, 100), 243(10), 149(17) 133(13), 112(76), 85 (11); HRMS calcd for $C_{14}H_{13}ON_3S$ 271.07738 found 271.07744; anal. calcd for $C_{14}H_{13}ON_3S$: C, 61.92; H, 4.83; N, 15.49; S, 11.82 found: C, 62.07; H, 5.03; N, 15.01; S, 12.01.

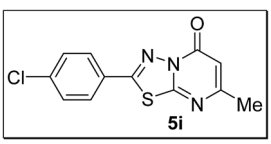

7-Methyl-2-(4-chlorophenyl)-5*H*-1,3,4-thiadiazolo[3,2-*a*]-pyrimidin-5-one (5i). According to the general procedure, using 4-chlorophenylboronic acid afforded 74 mg of product **5a** (65%); brown solid; mp (204–205 °C); ^{1}H NMR (250 MHz, $CDCl_3$) δ 7.91 (d, ^3J = 8.66 Hz, 2H, CH_{Ar}), 7.51 (d, ^3J = 8.57 Hz, 2H, CH_{Ar}), 6.34 (s, 1H, $CH_{Het\text{-}Ar}$), 2.41 (s, 3H, CH_3); ^{13}C NMR (62 MHz, $CDCl_3$) δ 162.97 (C_{Ar}), 160.76 (C_{Ar}), 156.76 (C_{Ar}), 139.48 (C_{Ar}), 129.81 (C_{Ar}), 128.93 (C_{Ar}), 128.44 (CH_{Ar}), 126.71 (CH_{Ar}), 107.90 ($CH_{Het\text{-}Ar}$), 23.69 (CH_3); IR (ATR) ν 3034 (w), 2962 (w), 2919 (w), 2850 (w), 1920 (w), 1787 (w), 1729 (w), 1695 (s), 1684 (s), 1569 (m), 1481 (s), 1390 (m), 1360 (w), 1085 (m), 833 (s), 691 (m), 573 (m) cm^{-1}; MS *m*/*z* 277 (M^+, 100), 249(16), 155(34), 140(11), 137(11), 112(87); HRMS calcd for $C_{12}H_8ON_3ClS$ 277.00711 found 277.00711; anal. calcd for $C_{12}H_8ON_3ClS$: C, 51.90; H, 2.90; N, 15.13; S, 11.55 found: C, 51.80; H, 2.44; N, 15.22; S, 11.78.

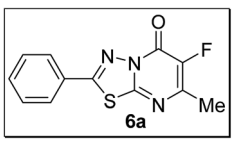

6-Fluoro-7-methyl-2-phenyl-5*H*-1,3,4-thiadiazolo[3,2-*a*]-pyrimidin-5-one (6a). According to the general procedure, using phenylboronic acid afforded 91 mg of product **6a** (92%); white solid; mp (206–207 °C); ^{1}H NMR (300 MHz, DMSO) δ 8.00 (d, ^3J = 6.75 Hz, 2H, CH_{Ar}), 7.64–7.71 (m, 3H, CH_{Ar}), 2.36 (d, ^4J = 2.64 Hz, 3H, CH_3); ^{13}C NMR (75 MHz, $CDCl_3$) δ 160.16 (C_{Ar}), 155.80 (d, ^4J = 3.35 Hz, CNNS), 150.36 (d, ^2J = 27.50 Hz, CO), 146.37 (d, ^2J = 16.85 Hz, *C*–CH_3), 144.41 (d, ^1J = 241.41 Hz, C–$F_{Het\text{-}Ar}$), 133.17 (CH_{Ar}), 129.76 (CH_{Ar}), 128.12 (C_{Ar}), 127.47 (CH_{Ar}), 17.11 (CH_3); IR (ATR) ν 3016 (w), 2967 (w), 2923 (w), 1720 (w), 1684 (s), 1585 (s), 1506 (s), 1482 (m), 1445 (m), 1362 (s), 1203 (s), 983 (m), 880 (m), 772 (s), 685 (s) cm^{-1}; MS *m*/*z* 261 (100), 130(10), 105(29), 89(10); HRMS calcd for $C_{12}H_8ON_3FS$ 261.03666 found 261.03655; anal. calcd for $C_{12}H_8ON_3FS$: C, 55.16; H, 3.09; N, 16.08; S; 12.27. Found: C, 54.87; H, 2.91; N, 15.83; S, 12.61.

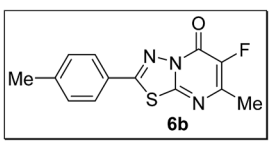

6-Fluoro-7-methyl-2-(4-methylphenyl)-5*H*-1,3,4-thiadiazolo [3,2-*a*]pyrimidin-5-one (6b). According to the general procedure, using 4-methylphenylboronic acid afforded 84 mg of product **6b** (80%); white solid; mp (270–271 °C); ^{1}H NMR (300 MHz, DMSO) δ 7.84 (d, ^3J = 8.35 Hz, 2H, CH_{Ar}), 7.33 (d, ^3J = 7.87 Hz, 2H, CH_{Ar}), 2.44 (s, 3H, CH_3), 2.43 (d, ^4J = 3.92 Hz, 3H, CH_3); ^{13}C NMR (62 MHz, $CDCl_3$) δ 159.95 (C_{Ar}), 154.13 (d, ^4J = 2.44 Hz, CNNS), 150.25 (d, ^2J = 27.42 Hz, CO), 146.11 (d, ^2J = 16.9 Hz, *C*–CH_3), 143.76 (d, ^1J = 247.65 Hz, C–$F_{Het\text{-}Ar}$), 143.36 (C_{Ar}), 129.29 (C_{Ar}), 126.85 (CH_{Ar}), 124.63 (CH_{Ar}), 20.85 (CH_3), 16.52 (CH_3); IR (ATR) ν 3043 (w), 2948 (w), 2923 (w), 1710 (w), 1692 (s), 1590 (s), 1514 (s), 1312 (s), 1217 (m), 1158 (m), 816 (s), 758 (m), 706 (m), 609 (s), 577 (s) cm^{-1}; MS *m*/*z* 275(100), 217(9), 135(15), 119(43); HRMS calcd for $C_{13}H_{10}ON_3FS$ 275.05221 found 275.05224; anal. calcd for $C_{13}H_{10}ON_3FS$: C, 56.72; H, 3.66; N, 15.26; S, 11.65. Found: C, 56.36; H, 3.74; N, 14.94; S, 11.24.

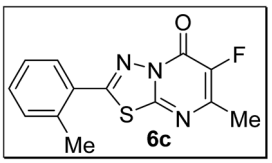

6-Fluoro-7-methyl-2-(2-methylphenyl)-1,3,4-5*H*-thiadiazolo[3,2-*a*]pyrimidin-5-one (6c). According to the general procedure, using 2-methylphenylboronic acid afforded 75 mg of product **6c** (72%); yellow solid; mp (170–171 °C); ^{1}H NMR (250 MHz, $CDCl_3$) δ 7.62 (d, ^3J = 7.87 Hz, 1H, CH_{Ar}), 7.46 (d, ^3J = 6.62 Hz, 1H, CH_{Ar}), 7.31–7.50 (m, 2H, CH_{Ar}), 2.68 (s, 3H, CH_3), 2.44 (d, ^4J = 3.77 Hz, 3H, CH_3); ^{13}C NMR (62 MHz, $CDCl_3$) δ 160.76 (C_{Ar}), 155.53 (d, ^2J = 28.93 Hz, CO), 155.26 (C_{Ar}), 150.85 (d, ^4J = 2.50 Hz, CNNS), 147.15 (d, ^2J = 17.01 Hz, *C*–CH_3), 144.88 (d, ^1J = 246.27 Hz, C–$F_{Het\text{-}Ar}$), 138.04 (C_{Ar}), 132.12 (CH_{Ar}), 130.42 (CH_{Ar}), 127.38 (CH_{Ar}), 126.65 (CH_{Ar}), 21.56 (CH_3), 17.45 (CH_3); IR (ATR) ν 2960 (w), 2925 (w), 2923 (w), 1707 (w), 1588 (s), 1504 (s), 1439 (w), 1207 (s), 1200 (m), 1170 (w), 880 (s), 764 (m), 755 (m), 710 (M), 625 (S) cm^{-1}; MS *m*/*z* 275(100), 217(8), 148(33), 144(12); HRMS calcd for $C_{13}H_{10}ON_3FS$ 275.05214 found 275.05231; anal. calcd for $C_{13}H_{10}ON_3FS$: C, 56.72; H, 3.66; N, 15.26; S, 11.65. Found: C, 56.57; H, 3.59; N, 15.47; S, 11.21.

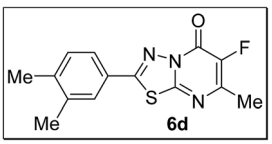

6-Fluoro-7-methyl-2-(3,4-dimethylphenyl)-5*H*-1,3,4-thiadiazolo[3,2-*a*]pyrimidin-5-one (6d). According to the general procedure, using 3,4-dimethylphenylboronic acid afforded 99 mg of product **6d** (92%); yellow solid; mp (218–219 °C); ^{1}H NMR (300 MHz, $CHCl_3$) δ 7.76 (d, ^4J = 2.07 Hz, 1H, CH_{Ar}), 7.62 (dd, ^3J = 7.84 Hz, ^4J = 2.02 Hz, 1H, CH_{Ar}), 7.26 (d, ^3J = 7.56 Hz, 1H, CH_{Ar}), 2.44 (d, ^4J = 3.77 Hz, 3H, CH_3), 2.34 (s, 6H, CH_3); ^{13}C NMR (75 MHz, $CDCl_3$) δ 160.88 (C_{Ar}), 154.90 (d, ^4J = 2.75 Hz, CNNS), 151.07 (d, ^2J = 27.43 Hz, CO), 146.95 (d, ^2J = 16.91 Hz, *C*–CH_3), 144.75 (d, ^1J = 246.39 Hz, C–$F_{Het\text{-}Ar}$), 142.86 (C_{Ar}), 138.09 (C_{Ar}), 130.47 (C_{Ar}), 128.35 (CH_{Ar}), 125.64 (CH_{Ar}), 125.28 (CH_{Ar}), 19.95 (CH_3), 19.49 (CH_3), 17.31 (CH_3); IR (ATR) ν 3048 (w), 2963 (w), 2927 (w), 1693 (s), 1586 (s), 1495 (m), 1209 (m), 1124 (w), 880 (m), 818 (m), 740 (m), 707 (m), 624 (w) cm^{-1}; MS *m*/*z* 289(100), 231(9), 149(15), 133(39); HRMS calcd for $C_{14}H_{12}ON_3FS$ 289.06788 found 289.06796; anal. calcd for $C_{14}H_{12}ON_3FS$: C, 58.12; H, 4.18; N, 14.52; S, 11.08 found: C, 58.82; H, 4.19; N, 14.44; S, 10.85.

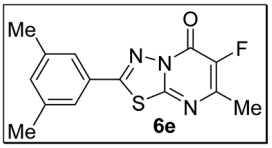

6-Fluoro-7-methyl-2-(3,5-dimethylphenyl)-5*H*-1,3,4-thiadiazolo[3,2-*a*]pyrimidin-5-one (6e). According to the general procedure, using 3,5-dimethylphenylboronic acid afforded 93 mg of product **6e** (85%); yellow solid; mp (271–272 °C); ^{1}H NMR (300 MHz, $CDCl_3$) δ 7.56 (s, 2H, CH_{Ar}), 7.22 (s, 1H, CH_{Ar}), 2.43 (d, ^4J = 3.84 Hz, 3H, CH_3), 2.39 (s, 6H, CH_3); ^{13}C NMR (75 MHz, $CDCl_3$) δ 161.13 (C_{Ar}), 155.03 (d, ^4J = 3.29 Hz, CNNS), 151.15 (d, ^2J = 27.65 Hz, CO), 147.08 (d, ^2J = 16.99 Hz, *C*–CH_3), 144.86 (d, ^1J = 246.71 Hz, C–$F_{Het\text{-}Ar}$), 139.40 (C_{Ar}), 134.97 (C_{Ar}), 128.01 (CH_{Ar}), 125.46 (CH_{Ar}), 21.09 (CH_3), 17.41 (CH_3); IR (ATR) ν 3029 (w), 2913 (w), 2859 (w), 1694 (s), 1589 (s), 1332 (m), 1211 (s), 1195 (m), 879 (m), 859 (m), 740 (m), 688 (m), 622 (w) cm^{-1}; MS *m*/*z* 289(100), 231(9), 149(15), 133(38); HRMS calcd for $C_{14}H_{12}ON_3FS$ 289.06796 found 289.06784; anal. calcd for $C_{14}H_{12}ON_3FS$: C, 58.12; H, 4.18; N, 14.52; S, 9.50. Found: C, 58.95; H, 4.38; N, 14.15; S, 9.81.

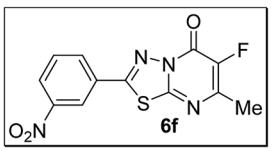

6-Fluoro-7-methyl-2-(3-nitrophenyl)-5*H*-1,3,4-thiadiazolo[3,2-*a*]pyrimidin-5-one (6f). According to the general procedure, using 3-nitrophenylboronic acid afforded 93 mg of product **6f** (84%); yellow solid; mp (225–226 °C); ^{1}H NMR (300 MHz, $CHCl_3$) 8.73 (pt, ^4J = 1.89 Hz, 1H, CH_{Ar}), 8.44–8.48 (m, 1H, CH_{Ar}), 8.34–8.37 (m, 1H, CH_{Ar}), 7.78 (pt, ^3J = 8.05 Hz, 1H, CH_{Ar}), 2.44 (d, ^4J = 3.90 Hz, 3H, CH_3); ^{13}C NMR (75 MHz, $CDCl_3$) δ 158.31 (C_{Ar}), 154.43 (d, ^4J = 3.24 Hz, CNNS), 151.09 (d, ^2J = 27.98 Hz, CO), 148.89 (C_{Ar}), 147.67 (d, ^2J = 17.09 Hz, *C*–CH_3), 145.11 (d, ^1J = 247.58 Hz, C–$F_{Het\text{-}Ar}$), 133.16 (C_{Ar}), 130.97 (CH_{Ar}), 130.05 (CH_{Ar}), 127.51 (CH_{Ar}), 122.75 (CH_{Ar}), 17.62 (CH_3); IR (ATR) ν 3095 (w), 3064 (w), 2959 (w), 1693 (s), 1582 (s), 1476 (m), 1274 (m), 1295 (m), 1106 (m), 916 (m), 738 (s), 681 (m), 626 (w) cm^{-1}; MS *m*/*z* 306(100), 276(9), 248(8), 150 (18), 144(12); HRMS calcd for $C_{12}H_7ON_4FS$ 306.02174 found 306.02164; anal. calcd for $C_{12}H_7ON_4FS$: C, 47.06; H, 2.30; N, 18.29; S, 10.47. Found: C, 46.95; H, 2.41; N, 17.99; S, 10.51.

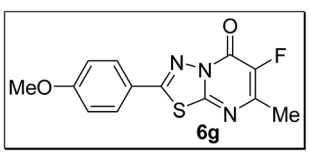

6-Fluoro-7-methyl-2-(4-methoxyphenyl)-5*H*-1,3,4-thiadiazolo[3,2-*a*]pyrimidin-5-one (6g). According to the general procedure, using 4-methoxyphenylboronic acid afforded 97 mg of product **6g** (88%); yellow solid; mp (206–207 °C); ^{1}H NMR (300 MHz, $CDCl_3$) δ 7.89 (d, ^3J = 8.88 Hz, 2H, CH_{Ar}), 7.01 (d, ^3J = 8.87 Hz, 2H, CH_{Ar}), 3.89 (s, 3H, OCH_3) 2.42 (d, ^4J = 3.81 Hz, 3H, CH_3); ^{13}C NMR (75 MHz, $CDCl_3$) δ 163.73 (C_{Ar}), 160.46 (C_{Ar}), 155.14 (d, ^4J = 3.33 Hz, CNNS), 151.30 (d, ^2J = 27.31 Hz, CO), 147.08 (d, ^2J = 17.08 Hz, *C*–CH_3), 145.05 (d, ^1J = 246.49 Hz, C–$F_{Het\text{-}Ar}$), 129.72 (C_{Ar}), 120.83 (CH_{Ar}), 115.00 (CH_{Ar}), 55.82 (OMe), 17.56 (CH_3); IR (ATR) ν 2961 (w), 2843 (w), 1698 (s), 1591 (s), 1498 (s), 1312 (s), 1254 (s), 1015 (m), 806 (s), 739 (m), 587 (m) cm^{-1}; MS *m*/*z* 291(100), 233(9), 136(12), 135(59), 133(9), 108(12);

HRMS calcd for $C_{13}H_{10}O_2N_3FS$ 291.04723 found 291.04772; anal. calcd for $C_{13}H_{10}O_2N_3FS$: C, 53.60; H, 3.46; N, 14.42; S, 11.01. Found: C, 53.29; H, 3.32; N, 13.98; S, 11.46.

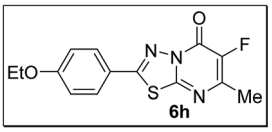

6-Fluoro-7-methyl-2-(4-ethoxyphenyl)-5*H*-1,3,4-thiadiazolo[3,2-*a*]pyrimidin-5-one (6h). According to the general procedure, using 4-ethoxyphenylboronic acid afforded 86 mg of product **6h** (75%); yellow solid; mp (185–186 °C); ^{1}H NMR (300 MHz, DMSO) δ 7.89 (d, ^3J = 8.87 Hz, 2H, CH_{Ar}), 7.12 (d, ^3J = 8.87 Hz, 2H, CH_{Ar}), 4.13 (q, ^3J = 7.07 Hz, 2H, OCH_2), 2.32 (d, ^4J = 3.84 Hz, 3H, CH_3), 1.35 (t, ^3J = 6.93 Hz, 3H, CH_3); ^{13}C NMR (75 MHz, $CDCl_3$) δ 162.21 (C_{Ar}), 159.62 (C_{Ar}), 155.63 (d, ^4J = 2.92 Hz, CNNS), 150.19 (d, ^2J = 27.85 Hz, CO), 146.92 (d, ^2J = 16.85 Hz, *C*–CH_3), 144.29 (d, ^1J = 241.27 Hz, C–$F_{Het\text{-}Ar}$), 129.24 (CH_{Ar}), 120.16 (CH_{Ar}), 115.40 (C_{Ar}), 63.70 (OCH_2), 16.96 (CH_3), 14.36 (CH_3); IR (ATR) ν 3085 (w), 2982 (w), 2934 (w), 2867 (w), 1698 (s), 1589 (s), 1514 (m), 1320 (m), 121 (m), 1176 (m), 844 (s), 743 (m), 706 (s), 607 (s), 569 (m) cm^{-1}; MS *m*/*z* 305(100), 217(9), 135(15), 119(43); HRMS calcd for $C_{14}H_{12}O_2N_3FS$ 305.0707 found 305.07063; anal. calcd for $C_{14}H_{12}O_2N_3FS$: C, 55.07; H, 3.96; N, 13.76; S, 10.50. Found: C, 55.36; H, 3.74; N, 13.25; S, 11.03.

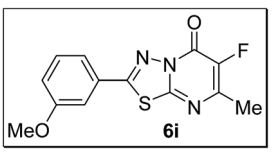

6-Fluoro-7-methyl-2-(3-methoxyphenyl)-5*H*-1,3,4-thiadiazolo[3,2-*a*]pyrimidin-5-one (6i). According to the general procedure, using 3-methoxyphenylboronic acid afforded 76 mg of product **6i** (70%); yellow solid; mp (202–203 °C); ^{1}H NMR (250 MHz, $CDCl_3$) δ 7.51–7.53 (m, 1H, CH_{Ar}), 7.44–7.41 (m, 2H, CH_{Ar}), 7.09–7.17 (m, 1H, CH_{Ar}), 3.90 (s, 3H, OCH_3) 2.43 (d, ^4J = 3.94 Hz, 3H, CH_3); ^{13}C NMR (62 MHz, $CDCl_3$) δ 160.48 (C_{Ar}), 160.12 (C_{Ar}), 154.75 (d, ^4J = 3.41 Hz, CNNS), 150.97 (d, ^2J = 27.73 Hz, CO), 147.02 (d, ^2J = 17.03 Hz, *C*–CH_3), 144.72 (d, ^1J = 246.73 Hz, C–$F_{Het\text{-}Ar}$), 130.34 (C_{Ar}), 129.25 (CH_{Ar}), 120.30 (CH_{Ar}), 119.52 (CH_{Ar}), 111.74 (CH_{Ar}), 55.61 (OMe), 17.28 (CH_3); IR (ATR) ν 3066 (w), 3023 (w), 2960 (w), 2940 (w), 2833 (w), 1694 (s), 1587 (s), 1328 (m), 1205 (s), 1032 (m), 833 (m), 800 (m), 786 (m), 679 (s), 626 (s) cm^{-1}; MS *m*/*z* 291(100), 217(9), 135(42), 133(9); HRMS calcd for $C_{13}H_{10}O_2N_3FS$ 291.04723 found 291.04695; anal. calcd for $C_{13}H_{10}O_2N_3FS$: C, 53.60; H, 3.46; N, 14.42; S, 11.01. Found: C, 53.31; H, 3.22; N, 14.28, S, 11.09.

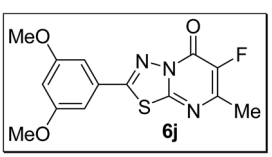

6-Fluoro-7-methyl-2-(3,5-dimethoxyphenyl)-5*H*-1,3,4-thiadiazolo[3,2-*a*]pyrimidin-5-one (6j). According to the general procedure, using 3,5-dimethoxyphenylboronic acid afforded 103 mg of product **6j** (85%); yellow solid; mp (264–265 °C); ^{1}H NMR (300 MHz, $CHCl_3$) 7.05 (d, ^4J = 2.25 Hz, 2H, CH_{Ar}), 6.66 (pt, ^4J = 2.29 Hz, 1H, CH_{Ar}), 3.87 (s, 6H, OCH_3), 2.43 (d, ^4J = 3.96 Hz, 3H, CH_3); ^{13}C NMR (75 MHz, $CDCl_3$) δ 160.45 (C_{Ar}), 159.81 (C_{Ar}), 153.18 (d, ^4J = 2.92 Hz, CNNS), 149.81 (d, ^2J = 28.60 Hz, CO), 146.23 (d, ^2J = 17.05 Hz, *C*–CH_3), 143.90 (d, ^1J = 246.48 Hz, C–$F_{Het\text{-}Ar}$), 128.90 (CH_{Ar}), 104.72 (CH_{Ar}), 104.30 (C_{Ar}), 54.90 (2 OCH_3), 16.46 (CH_3); IR (ATR) ν 3077 (w), 3025 (w), 2958 (w), 1695 (s), 1589 (s), 1458 (m), 1301 (m), 1185 (m), 1085 (m), 897 (m), 813 (s), 750 (m), 622 (w) cm^{-1}; MS *m*/*z* 321(100), 165(47), 144(4), 123 (7), 122(4); HRMS calcd for $C_{14}H_{12}O_3N_3FS$ 321.05779 found 321.05762; anal. calcd for $C_{14}H_{12}O_3N_3FS$: C, 52.33; H, 3.76; N, 13.08; S, 9.98. Found: C, 52.50; H, 3.76; N, 12.03; S, 9.81.

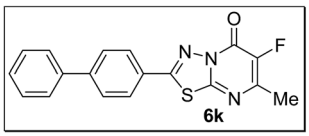

6-Fluoro-7-methyl-2-(4-phenylphenyl)-5*H*-1,3,4-thiadiazolo[3,2-*a*]pyrimidin-5-one (6k). According to the general procedure, using 4-phenylphenylboronic acid afforded 80 mg of product **6k** (62%); yellow solid; mp (284–285 °C); ^{1}H NMR (300 MHz, $CHCl_3$) 8.03 (d, ^3J = 8.49 Hz, 2H, CH_{Ar}), 7.75 (d, ^3J = 8.49 Hz, 2H, CH_{Ar}), 7.63–7.66 (m, 2H, CH_{Ar}), 7.42–7.52 (m, 3H, CH_{Ar}), 2.44 (d, ^4J = 3.77 Hz, 3H, CH_3); ^{13}C NMR (62 MHz, $CDCl_3$) δ 159.48 (C_{Ar}), 153.99 (d, ^4J = 3.08 Hz, CNNS), 150.21 (d, ^2J = 27.85 Hz, CO), 146.18 (d, ^2J = 17.02 Hz, *C*–CH_3), 145.14 (C_{Ar}), 144.01 (d, ^1J = 243.56 Hz, C–$F_{Het\text{-}Ar}$), 138.31 (C_{Ar}), 128.18 (C_{Ar}), 127.68 (CH_{Ar}), 127.31 (CH_{Ar}), 127.06 (CH_{Ar}), 126.27 (CH_{Ar}), 126.02 (CH_{Ar}), 16.51 (CH_3); IR (ATR) ν 3056 (w), 3032 (w), 2961 (w), 1691 (s), 1590 (m), 1507 (m), 1274 (m), 1290 (m), 877 (m), 841 (m), 762 (s), 743 (m), 688 (m) cm^{-1}; MS *m*/*z* 337(100), 284(15), 197(13), 181(44), 152(17), 144(5); HRMS calcd for $C_{18}H_{12}ON_3FS$ 337.06796 found 337.06774; anal. calcd for $C_{18}H_{12}ON_3FS$: C, 64.08, H, 3.59; N, 12.46; S, 9.50. Found: C, 63.59; H, 3.68; N, 12.50; S, 9.43.

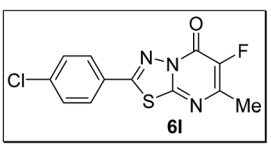

6-Fluoro-7-methyl-2-(4-chlorophenyl)-5*H*-1,3,4-thiadiazolo[3,2-*a*]pyrimidin-5-one (6l). According to the general procedure, using 4-chlorophenylboronic acid afforded 80 mg of product **6j** (72%); white solid; mp (260–261 °C); ^{1}H NMR (300 MHz, $CDCl_3$) δ 7.88 (d, ^3J = 8.70 Hz, 2H, CH_{Ar}), 7.51 (d, ^3J = 8.70 Hz, 2H, CH_{Ar}), 2.42 (d, ^4J = 3.87 Hz, 3H, CH_3); ^{13}C NMR (75 MHz, $CDCl_3$) δ 159.58 (C_{Ar}), 154.80 (d, ^4J = 3.04 Hz, CNNS), 151.15 (d, ^2J = 28.06 Hz, CO), 147.38 (d, ^2J = 17.03 Hz, *C*–CH_3), 145.84 (d, ^1J = 247.27 Hz, C–$F_{Het\text{-}Ar}$), 139.77 (C_{Ar}), 129.96 (C_{Ar}), 129.02 (CH_{Ar}), 126.81 (CH_{Ar}), 17.57 (CH_3); IR (ATR) ν

3067 (w), 2962 (w), 2921 (w), 1752 (w), 1696 (s), 1586 (s), 1510 (s), 1483 (m), 1404 (m), 1219 (m), 1090 (s), 1011 (m), 841 (s), 743 (s), 606 (m) cm^{-1}; MS *m*/*z* 295(100), 237(8), 155(23), 139(35); HRMS calcd for $C_{12}H_7ON_3ClFS$ 294.9976 found 294.9976; anal. calcd for $C_{12}H_7ON_3ClF$: C, 48.74; H, 2.39; N, 14.21; S, 10.84. Found: C, 48.34; H, 2.68; N, 13.93; S, 11.01.

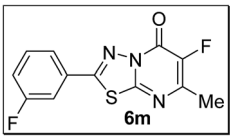

6-Fluoro-7-methyl-2-(4-fluorophenyl)-5*H*-1,3,4-thiadiazolo[3,2-*a*]pyrimidin-5-one (6m). According to the general procedure, using 4-fluorophenylboronic acid afforded 93 mg of product **6m** (88%); yellow solid; mp (213–214 °C); ^{1}H NMR (300 MHz, $CHCl_3$) δ 7.68–7.74 (m, 2H, CH_{Ar}), 7.48–7.56 (m, 1H, CH_{Ar}), 7.28–7.34 (m, 1H, CH_{Ar}), 2.43 (d, ^4J = 3.87 Hz, 3H, CH_3); ^{13}C NMR (75 MHz, $CDCl_3$) δ 162.66 (d, ^1J = 249.79 Hz, C–F_{Ar}), 159.01 (d, ^4J = 3.30 Hz, C_{Ar}), 154.35 (d, ^4J = 2.75 Hz, CNNS), 150.73 (d, ^2J = 28.05 Hz, CO), 147.02 (d, ^2J = 17.06 Hz, *C*–CH_3), 144.63 (d, ^1J = 247.30 Hz, C–$F_{Het\text{-}Ar}$), 131.00 (d, ^3J = 8.25 Hz, C_{Ar}), 129.01 (d, ^3J = 8.21 Hz, CH_{Ar}), 123.36 (d, ^4J = 3.25 Hz, CH_{Ar}), 119.96 (d, ^2J = 21.45 Hz, CH_{Ar}), 114.29 (d, ^2J = 24.21 Hz, CH_{Ar}), 17.16 (CH_3); IR (ATR) ν 3082 (w), 2961 (w), 2918 (w), 1699 (s), 1587 (s), 1479 (m), 1208 (m), 1181 (w), 883 (m), 846 (m), 788 (s), 742 (s), 683 (s) cm^{-1}; MS *m*/*z* 279(100), 221(11), 144(11), 139(29); HRMS calcd for $C_{12}H_7ON_3F_2S$ 279.02724 found 279.02739; anal. calcd for $C_{12}H_7ON_3F_2S$: C, 51.61; H, 2.53; N, 15.05; S, 11.48. Found: C, 52.08; H, 2.54; N, 15.11; S, 11.42.

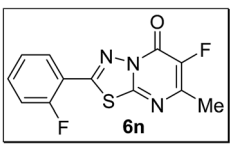

6-Fluoro-7-methyl-2-(2-fluorophenyl)-5*H*-1,3,4-thiadiazolo[3,2-*a*]pyrimidin-5-one (6n). According to the general procedure, using 2-fluorophenylboronic acid afforded 93 mg of product **6n** (88%); yellow solid; mp (217–218 °C); ^{1}H NMR (300 MHz, $CHCl_3$) δ 8.40 (ddd, ^3J = 7.58 Hz, ^3J = 7.68 Hz, ^4J = 1.64 Hz, 1H, CH_{Ar}), 7.57–7.64 (m, 1H, CH_{Ar}), 7.23–7.38 (m, 2H, CH_{Ar}), 2.44 (d, ^4J = 3.87 Hz, 3H, CH_3); ^{13}C NMR (62 MHz, $CDCl_3$) δ 162.79 (d, ^2J = 20.10 Hz, C_{Ar}), 162.05 (d, ^3J = 9.37 Hz, C_{Ar}), 156.69 (d, ^1J = 258.34 Hz, C–F_{Ar}), 147.63 (d, ^2J = 16.98 Hz, *C*–CH_3), 144.78 (d, ^1J = 246.27 Hz, C–$F_{Het\text{-}Ar}$), 139.87 (d, ^4J = 4.57 Hz, CNNS), 136.07 (d, ^2J = 29.75 Hz, CO), 134.95 (d, ^3J = 8.69 Hz, CH_{Ar}), 129.01 (d, ^5J = 1.37 Hz, CH_{Ar}), 125.43 (d, ^4J = 3.50 Hz, CH_{Ar}), 116.65 (d, ^2J = 21.20 Hz, CH_{Ar}), 17.65 (CH_3); IR (ATR) ν 3066 (w), 3041 (w), 2960 (w), 1698 (s), 1585 (s), 1451 (m), 1288 (m), 1159 (w), 884 (m), 874 (m), 778 (s), 744 (s), 623 (m), 613 (m) cm^{-1}; MS *m*/*z* 279(100), 221(12), 144(12), 139(32); HRMS calcd for $C_{12}H_7ON_3F_2S$ 279.03507 found 279.03506; anal. calcd for $C_{12}H_7ON_3F_2S$: C, 51.61; H; 2.53; N; 15.05, S; 11.48. Found: C, 51.88; H, 2.48; N, 14.83; S, 11.13.

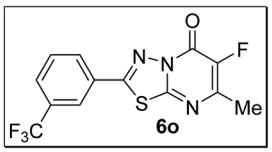

6-Fluoro-7-methyl-2-(3-trifluoromethylphenyl)-5*H*-1,3,4-thiadiazolo[3,2-*a*]pyrimidin-5-one (6o). According to the general procedure, using 3-trifluoromethylphenylboronic acid afforded 90 mg of product **6o** (72%); yellow solid; mp (163–164 °C); ^{1}H NMR (300 MHz, $CHCl_3$) 8.21 (s, 1H, CH_{Ar}), 8.13 (d, ^3J = 8.16 Hz, 1H, CH_{Ar}), 7.87 (d, ^3J = 8.02 Hz, 1H, CH_{Ar}), 7.70 (d, ^3J = 7.85 Hz, 1H, CH_{Ar}), 2.44 (d, ^4J = 4.02 Hz, 3H, CH_3); ^{13}C NMR (62 MHz, $CDCl_3$) δ 158.96 (C_{Ar}), 154.34 (q, ^4J = 2.74 Hz, C_{Ar}), 150.88 (d, ^2J = 27.91 Hz, CO), 147.28 (d, ^2J = 16.93 Hz, *C*–CH_3), 144.82 (d, ^1J = 247.65 Hz, C–$F_{Het\text{-}Ar}$), 132.14 (q, ^2J = 33.43 Hz, C_{Ar}), 130.74 (q, ^5J = 0.84 Hz, C_{Ar}), 130.06 (CH_{Ar}), 129.47 (q, ^3J = 3.62 Hz, CH_{Ar}), 128.99 (CH_{Ar}), 124.35 (q, ^3J = 3.81 Hz, CH_{Ar}), 123.08 (q, ^1J = 272.62 Hz, CF_3), 17.32 (CH_3); IR (ATR) ν 3086 (w), 2921 (w), 2850 (w), 1696 (s), 1588 (s), 1430 (m), 1259 (m), 1173 (w), 879 (m), 826 (m), 760 (s), 743 (m), 693 (s) cm^{-1}; MS *m*/*z* 329(100), 271(11), 189(25), 173(32); HRMS calcd for $C_{13}H_7ON_3F_4S$ 329.02405 found 329.02371; anal. calcd for $C_{13}H_7ON_3F_4S$: C, 47.42; H, 2.14; N, 12.76; S, 9.74. Found: C, 48.04; H, 2.37; N, 13.03; S, 10.01.

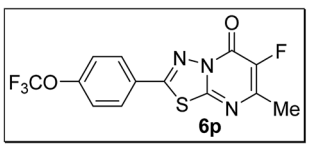

6-Fluoro-7-methyl-2-(4-trifluoromethoxyphenyl)-5*H*-1,3,4-thiadiazolo[3,2-*a*]pyrimidin-5-one (6p). According to the general procedure, using 3-trifluoromethoxyphenyl boronic acid afforded 65 mg of product **6p** (50%); yellow solid; mp (229–230 °C); ^{1}H NMR (300 MHz, $CHCl_3$) 8.01 (d, ^3J = 8.88 Hz, 2H, CH_{Ar}), 7.37 (d, ^3J = 8.37 Hz, CH_{Ar}, 2H, CH_{Ar}), 7.70 (d, ^3J = 7.85 Hz, 2H, CH_{Ar}), 2.43 (d, ^4J = 3.77 Hz, 3H, CH_3); ^{13}C NMR (62 MHz, $CDCl_3$) δ 159.15 (C_{Ar}), 154.69 (C_{Ar}), 152.62 (q, ^3J = 2.09 Hz, C_{Ar}), 151.09 (d, ^2J = 27.92 Hz, CO), 147.34 (d, ^2J = 17.13 Hz, *C*–CH_3), 144.97 (d, ^1J = 247.19 Hz, C–$F_{Het\text{-}Ar}$), 129.59 (C_{Ar}), 124.49 (q, ^1J = 270.16 Hz, OCF_3), 121.45 (q, ^4J = 0.91 Hz, CH_{Ar}), 118.21 (CH_{Ar}), 17.47 (CH_3); IR (ATR) ν 3046 (w), 2960 (w), 2918 (w), 1695 (s), 1590 (s), 1515 (m), 1273 (m), 1170 (w), 853 (m), 846 (m), 731 (w), 743 (m), 680 (w) cm^{-1}; MS *m*/*z* 345(100), 284(15), 189(42), 144(12); HRMS calcd for $C_{13}H_7ON_3F_4S$ 345.01896 found 345.01863; anal. calcd for $C_{13}H_7ON_3F_4S$: C, 45.22; H, 2.04; N, 12.17; S, 9.29. Found: C, 45.04; H, 2.37; N, 12.03; S, 9.01.

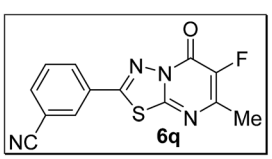

6-Fluoro-7-methyl-2-(3-cyanophenyl)-5*H*-1,3,4-thiadiazolo[3,2-*a*]pyrimidin-5-one (6q). According to the general procedure, using 3-cyanophenyl boronic acid afforded 83 mg of product **6q** (77%); white solid; mp (210–211 °C); ^{1}H NMR (300 MHz, $CHCl_3$)

δ 8.19–8.25 (m, 2H, CH_{Ar}), 7.88–7.91 (m, 1H, CH_{Ar}), 7.68–7.73 (m, 1H, CH_{Ar}), 2.44 (d, ^4J = 3.78 Hz, 3H, CH_3); ^{13}C NMR (62 MHz, $CDCl_3$) δ 156.37 (d, ^1J = 247.79 Hz, C–$F_{Het\text{-}Ar}$), 150.85 (C_{Ar}), 147.62 (d, ^2J = 17.11 Hz, *C*–CH_3), 143.12 (CH_{Ar}), 140.04 (d, ^2J = 28.37 Hz, CO), 136.11 (C_{Ar}), 131.59 (C_{Ar}), 131.08 (CH_{Ar}), 130.63 (CH_{Ar}), 129.73 (CH_{Ar}), 117.15 (CH_{Ar}), 114.38 (CN), 17.60 (CH_3); IR (ATR) ν 3054 (w), 3031 (w), 2917 (w), 1694 (s), 1592 (s), 1483 (m), 1288 (m), 1155 (w), 884 (m), 805 (m), 761 (s), 744 (s), 684 (s), 628 (m) cm^{-1}; MS *m*/*z* 286(100), 228(12), 146(23), 130(43), 128(46), 102(17); HRMS calcd for $C_{13}H_7ON_4FS$ 279.03507 found 279.03506; anal. calcd for $C_{13}H_7ON_4FS$: C, 54.54; H, 2.46; N, 19.57; S, 11.20. Found: C, 54.61; H, 2.46; N, 19.01; S, 10.88.

Biological protocols

Cell transfection with human NPPs. The plasmids expressing human NPPs ((NPP1)[35] or (NPP3)[36]) or human NTPDases ((NTPDase 1)[37] or (NTPDase 2)[38]) or (NTPDase 3)[39] or (NTPDase 8)[40] were transfected with COS-7 in 10 cm plates using Lipofectamine, as previously reported.[41] The confluent cells (80–90%) were incubated at 37 °C for 5 h, in Dulbecco's modified Eagle's medium (DMEM) (without fetal bovine serum (FBS)) with 6 μg of plasmid DNA and 24 μL of Lipofectamine reagent. At the end, transfection was stopped by adding same volume of DMEM/F-12 containing 20% FBS and cells were harvested 40–72 h later.

Preparation of membrane fractions. For the preparation of protein extracts, the transfected cells were washed trice with Tris-saline buffer (4 °C). Then cells were collected by scraping in the harvesting buffer (95 mM NaCl, 0.1 mM PMSF and 45 mM Tris at pH 7.5) and washed two times by centrifugation at 300 × *g* for 5 min at 4 °C.[41] The obtained cells were resuspended in the harvesting buffer containing 10 μg μL^{-1} aprotinin and then sonicated. Cellular debris and nucleus were separated out by 10 min centrifugation (300 × *g* at 4 °C). The supernanent (crude protein extract) was aliquoted and kept at −80 °C until used for activity assay. Protein concentration was estimated by using Bradford microplate assay[42] using bovine serum albumin as a reference standard.

Nucleoside triphosphate diphosphohydrolase inhibition assay

The inhibitory effect of all the derivatives on nucleoside triphosphate diphosphohydrolase (h-NTPDase1, 2, 3 & 8) were performed by doing slight modifications in previously reported spectrophotometric method.[43] The assay was carried out in reaction buffer *i.e.* 500 mM Tris–HCl buffer (pH 7.4). All the synthetic compounds were tested at the final concentration of 0.5 mM (with final DMSO 1% (v/v)). The total assay volume of 100 μL contained 45 μL of the Tris-buffer, 10 μL of tested compound followed by the addition of 10 μL of h-NTPDase1 (58 ng of protein per well) or 10 μL of h-NPDase 2 (79 ng of protein per well) or 10 μL h-NTPDase 3 (163 ng of protein per well) or 10 μL h-NTPDase 8(66 ng of protein per well). The reaction mixture was incubated for 10 minutes at 37 °C and absorbance was measured at 630 nm using microplate reader (BioTek ELx800, Instruments, Inc. USA). Then, 10 μL of adenosine triphosphate (ATP) substrate was added at a final concentration of 0.5 mM. The reaction mixture was again incubated at 37 °C for 20 minutes and then 25 μL of malachite green reagent was added. Change in the absorbance was measured after 6–8 min. The compounds which exhibited over 50% inhibition of any isoform of NTPDase activity were further evaluated for determination of IC_{50} values. All experiments were carried out in triplicate. The IC_{50} values were determined by using non-linear curve fitting program PRISM 5.0 (GraphPad, San Diego, California, USA).

Nucleotide pyrophosphatase inhibition assay

The inhibitory effect of all the derivatives on nucleotide pyrophosphatase (h-NPP1 & h-NPP3) was carried out according to our previously reported method.[44] The reaction buffer used for this assay was consisted of 5 mM $MgCl_2$, 0.1 mM $ZnCl_2$, 50 mM Tris–HCl (pH 9.5) and 25% glycerol. To the total assay volume of 100 μL, 10 μL of tested compound solution was added (at 0.1 mM final concentration) followed by the addition of 10 μL of h-NPP1 (final conc. of 27 ng) or h-NPP3 (final conc. of 25 ng). The reaction mixture was allowed to incubate for 10 min at 37 °C and absorbance was measured at 405 nm using microplate reader (BioTek ELx800, Instruments, Inc. USA). Then 10 μL of substrate *p*-nitrophenyl-5′-thymidine monophosphate (*p*-Nph-5-TMP, 0.5 mM) was added to initiate the reaction and the mixture was allowed to incubate 37 °C. The change in absorbance was measured after 30 min. The compounds which exhibited over 50% inhibition of enzyme activity were further selected for evaluation of IC_{50} values. All experiments were carried out in triplicate. The IC_{50} values were calculated by using non-linear regression analysis of program PRISM 5.0 (GraphPad, San Diego, California, USA).

Mechanism of inhibition. To further characterize the interaction of most potent inhibitors of h-NPP1 and h-NPP3, the type of inhibition was determined by Michaelis–Menten kinetics. For this purpose, the initial rates of the enzyme inhibition at four different substrate concentrations (125 μM, 250 μM, 500 μM and 750 μM) in the absence and in the presence of four different concentrations (0 μM, 0.50 μM, 1.00 μM and 2.00 μM) of the selected representative inhibitor **6e** against h-NPP1 and **6j** against h-NPP3 were measured. The results are illustrated as double reciprocal Lineweaver–Burk plots in Fig. 4 and 5.

Homology modelling of human NPP1 and NPP3

Homology modelling of target proteins that is h-NPP1 and h-NPP3 was carried out using MOE (2014.0901) package. Amino acid sequence of h-NPP1 and h-NPP3 were downloaded from NCBI protein database. UniprotKB/Swiss-prot ID P22413 of h-NPP1 and accession code O14638 for human NPP3 were retrieved from NCBI protein data bank and loaded to MOE. Identification of suitable template protein structures were investigated by BLOSUM62 and then incorporated in MOE package.[33] X-rays crystallographic structure of mouse Enpp1 (PDB ID 4B56) from rcsb protein data bank[32] was used as a template structure for homology modelling of our target proteins. Total ten homology models of target protein were generated. Among these ten model structures one best model

was selected and refined using Amber12:EHT[45,46] force field. The protonation of the model proteins was also carried out using built-in Protonate-3D tool in MOE. Validation and comparison of homology models with the X-ray tempale structure was performed by re-aligning and superimposing with each other. Align sequence and structural alignment utilities of MOE were used for aligning and sequencing the modelled proteins with template protein. The RMSD values for modelled proteins were find out and Ramachandran plots were generated for both modelled proteins (see ESI†).

Molecular docking studies. Molecular docking of the most active inhibitor **6e** and **6j** of h-NPP1 and h-NPP3 respectively, were performed to find out the putative binding mode in the active site of modelled enzymes. Firstly, the chemical structures of the most potent compounds were generated using builder tool and then 3D optimized in Molecular Operating Environment (MOE) 2014, 09 software.[33] Prior to molecular docking studies protonation and energy minimization of all modelled structures of both targets were performed using MOE. After prerequisite preparation of inhibitors as well as target enzymes AutoDock4 and AutoDock Tool were used to perform molecular docking studies.

Grid box having dimension of $60 \times 60 \times 60$ in *XYZ* direction was built over both targets and centroid on the active site of target enzymes. Lamarckian genetic algorithm (LGA) was used as docking search parameter. The number of GA runs was set to 50 and number of maximum evaluation was 5×10^6. After successful completion of docking, pdbqt files were then converted into pdb files using OpenBabel.[47] Best pose having lowest free binding energy was selected for visualization of putative binding mode inside active site of target protein. Discovery Studio Visualizer v4.0 was used for visual inspection of putative binding interactions.[48]

Acknowledgements

We are grateful to the DAAD (Programm Deutsch-Pakistanische Hochschulzusammenarbeit) for financial support. J. Iqbal is thankful to the Organization for the Prohibition of Chemical Weapons (OPCW), The Hague, The Netherlands and Higher Education Commission of Pakistan for the financial support through Project No. 20-3733/NRPU/R&D/14/520 for the financial support. J. S. was supported by grants from the Canadian Institutes of Health Research. J. S. is also a recipient of a "Chercheur National" Scholarship award from the "Fonds de recherche du Québec-Santé" (FRQS).

References

1 A. M. Cardoso, M. R. C. Schetinger, P. Correia de Sá and J. Sévigny, *Auton. Neurosci.*, 2015, **191**, 25.
2 C. Stefan, S. Jansen and M. Bollen, *Purinergic Signalling*, 2006, **2**, 361.
3 G. Burnstock, *Curr. Top. Med. Chem.*, 2004, **4**, 793.
4 (*a*) J. M. Rhett, S. A. Fann and M. J. Yost, *Tissue Eng., Part B*, 2004, **20**(5), 392; (*b*) J. M. Rhett, S. A. Fann and M. J. Yost, *Tissue Eng., Part B*, 2004, **20**(5), 392.
5 (*a*) M. P. Abbracchio, G. Burnstock, A. Verkhratsky and H. Zimmermann, *Trends Neurosci.*, 2009, **32**, 19; (*b*) M. P. Abbracchio, G. Burnstock, A. Verkhratsky and H. Zimmermann, *Trends Neurosci.*, 2009, **32**(1), 19.
6 G. G. Yegutkin, *Biochim. Biophys. Acta*, 2008, **1783**(5), 673.
7 F. Kukulski, S. A. Lévesque and J. Sévigny, *Adv. Pharmacol.*, 2011, **61**, 263.
8 B. Atkinson, K. Dwyer, K. Enjyoji and S. C. Robson, *Blood Cells, Mol., Dis.*, 2006, **36**(2), 217.
9 (*a*) A. R. Beaudoin, J. Sevigny and M. Picher, in *Biomembranes*, ed. A. G. Lee, Jai Press, Greenwich, CT, 1996, vol. 5, pp. 369–401; (*b*) M. R. C. Schetinger, V. M. Morsch, C. D. Bonan and A. T. Wyse, *BioFactors*, 2007, **31**(2), 77.
10 É. G. Lavoie, F. Kukulski, S. A. Lévesque, J. Lecka and J. S. Vigny, *Biochem. Pharmacol.*, 2004, **67**, 1917.
11 F. Bigonnesse, S. A. Lévesque and F. Kukulski, *Biochemistry*, 2004, **43**, 5511.
12 T. F. Wang and G. Guidotti, *J. Biol. Chem.*, 1998, **273**, 11392.
13 A. Biederbick, C. Kosan, J. Kunz and H. P. Elsasser, *J. Biol. Chem.*, 2000, **275**, 19018.
14 A. Tokumura, E. Majima, Y. Kariya, K. Tominaga, K. Kogure, K. Yasuda and K. Fukuzawa, *J. Biol. Chem.*, 2002, **277**(42), 39436.
15 I. Aerts, J. J. Martin, P. P. De Deyn, C. Van Ginniken, X. Van Ostade, M. Kockx, G. Dua and H. Slegers, *Clin. Neurol. Neurosurg.*, 2011, **113**(3), 224.
16 S. Jansen, A. Perrakis, C. Ulens, C. Winkler, M. Andries, R. P. Joosten, M. Van Acker, F. P. Luyten, W. H. Moolenaar and M. Bollen, *Structure*, 2012, **20**(11), 1948.
17 J. W. Goding, B. Grobben and H. Slegers, *Biochim. Biophys. Acta*, 2003, **1638**(1), 1.
18 H. Younis, *Mini–Rev. Med. Chem.*, 2015, **15**, 21.
19 M. Al-Rashida and J. Iqbal, *Mini–Rev. Med. Chem.*, 2014, **34**(4), 703.
20 (*a*) R. A. Sabbadini and R. A. Sabbadini, Patent: US Application 2008/12/098, 2008, p. 419; (*b*) J. Iqbal, S. A. Lévesque, J. Sévigny and C. E. Müller, *Electrophoresis*, 2008, **29**, 3685; (*c*) L. Chang, S. Y. Lee, S. P. Leonczak, J. Rozenski, S. C. De Jonghe, T. Hanck, C. E. Müller and P. Herdewijn, *J. Med. Chem.*, 2014, **57**, 10080; (*d*) E. E. Shayhidin, E. Forcellini, M. C. Boulanger, A. Mahmut, S. Dautrey, X. Barbeau, P. Lagüe, J. Sévigny, J. F. Paquin and P. Mathieu, *Br. J. Pharmacol.*, 2015, **172**, 4189.
21 (*a*) V. Alagarsamy, U. S. Pathak, V. Rajasolomon, S. Meena, K. V. Ramseshu and R. Rajesh, *Indian J. Heterocycl. Chem.*, 2004, **13**, 347; (*b*) N. Terzioglu and A. Gursoy, *Eur. J. Med. Chem.*, 2003, **38**, 781; (*c*) E. A. El-Gaby, S. G. Abdel-Hamide, M. M. Ghorab and S. M. El-Sayed, *Acta Pharm.*, 1999, **49**, 149; (*d*) E. G. E. Devries, J. A. Gietma, P. Workman, J. E. Scott, A. Crawshaw, H. J. Dobbis, I. Dennis, N. Mulder, D. T. H. Sleijfer and P. H. B. Willemse, *Br. J. Cancer*, 1993, **68**, 661; (*e*) N. S. El-Sayed, E. R. El-Bendary, S.-M. El-Ashry and M. M. El-Kerdawy, *Eur. J. Med. Chem.*, 2011, **46**, 3714.
22 (*a*) J. G. J.-K. Jiang, J. McCoy, M. Shen, C. A. LeClair, W. Huang, A. Negri, J. Li, R. Blue, A. W. Harrington,

S. Naini, G. David III, W.-S. Choi, E. Volpi, J. Fernandez, M. Babayeva, M. A. Nedelman, M. Filizola, B. S. Coller and C. J. Thomas, *Bioorg. Med. Chem. Lett.*, 2014, **24**, 1148; (*b*) B. S. Coller, C. Thomas, M. Filizola, J. McCoy, W. Huang, M. Shen and J. K. Jiang, Patent: US 2015/0050325 A1, 2015.

23 (*a*) K. R. Sathisha, S. A. Khanum, J. N. N. S. Chandra, F. Ayisha, S. Balaji, G. K. Marathe, S. Gopal and K. S. Rangappa, *Bioorg. Med. Chem.*, 2011, **19**, 211; (*b*) M. Modica, M. Santagati, F. Russo, L. Parotti, L. De Gioia, C. Salvaggini, M. Salmona and T. Mennini, *J. Med. Chem.*, 1997, **40**, 574.

24 (*a*) B. V. Ashalatha, B. Narayana, K. K. V. Raj and N. S. Kumari, *Eur. J. Med. Chem.*, 2007, **42**, 719; (*b*) D. Ranganath, A. Mazumdar, S. Mulukuri, R. Doonaboina, M. Devarakonda and M. R. Prasad, *Med. Chem. Res.*, 2012, **21**, 2458; (*c*) S. Isoda, N. Suzuki, T. Miwa and S. Aibara, Patent: US1987/4652646, 1987; (*d*) S. Isoda, S. Aibara, T. Miwa, H. Fujiwara, S. Yokohama and H. Matsumoto, Patent: US1990/4898943, 1990.

25 (*a*) B. S. Coller, C. Thomas, M. Filizola, M. Joshua, W. Huang, M. Shen and J. K. Jiang, Patent: US2015/0050325Al, 2015; (*b*) R. Blue and B. S. Coller, Patent: US9,073,945B2, 2015.

26 (*a*) G. Kornis, P. J. Marks and C. G. Chidester, *J. Org. Chem.*, 1980, **45**, 4860; (*b*) T. Okabe, K. Maekawa and E. Taniguchi, *Agric. Biol. Chem.*, 1973, **35**(5), 1197; (*c*) M. A. Kukaniev and C. Párkányi, *J. Heterocycl. Chem.*, 2011, **48**, 1308.

27 (*a*) M. A. Kukaniev, U. Nurov, S. S. Shukurov and Y. Khodzhibaev, *Russ. Chem. Bull.*, 1999, **48**, 1143; (*b*) S. S. Shukurov, M. A. Kukaniev and M. A. Nasyrov, *Russ. Chem. Bull.*, 2004, **44**, 1957; (*c*) M. A. Kukaniev and C. Párkányi, *J. Heterocycl. Chem.*, 2011, **48**, 1308; (*d*) H.-R. Dong, Z.-L. Gao, R.-S. Li, Y.-M. Hu, H.-S. Dong and Z.-X. Xie, *RSC Adv.*, 2014, **4**, 55827.

28 (*a*) S. S. Shukurov and M. A. Kukaniev, *Khim. Geterotsikl. Soedin.*, 1992, **8**, 1148; (*b*) S. S. Shukurov, M. A. Kukaniev, M. A. Nasyrov, K. S. Zakharov and R. A. Karakhanov, *Russ. Chem. Bull.*, 1993, **42**, 1874; (*c*) S. S. Shukurov, M. A. Kukaniev, M. A. Nasyrov, K. S. Zakharov and R. A. Karakhanov, *Russ. Chem. Bull.*, 1994, **43**, 854; (*d*) S. S. Shukurov, M. A. Kukaniev, B. M. Bobogafirov and S. S. Sabirov, *Chem. Heterocycl. Compd.*, 1994, **30**, 127; (*e*) M. A. Kukaniev, S. S. Shukurov and M. A. Nasyrov, *Chem. Heterocycl. Compd.*, 1996, **32**, 479; (*f*) M. A. Kukaniev, U. Nurov, S. S. Shukurov and Yu. Khodzhibaev, *Russ. Chem. Bull.*, 1999, **48**, 1143; (*g*) T. M. Salimov, M. A. Kukaniev, I. T. Sattorov and D. M. Osimov, *Pharm. Chem. J.*, 2005, **39**, 311; (*h*) M. A. Kukaniev, T. M. Salimov, M. S. Murvatulloeva and I. K. Imatshoev, *Pharm. Chem. J.*, 2006, **40**, 421; (*i*) M. A. Kukaniev, M. D. Osimov, Z. G. Sangov, S. S. Safarov, M. B. Karimov and T. R. Radjabov, *Chem. Heterocycl. Compd.*, 2008, **44**, 882.

29 C. Copin, N. Henry, F. Buron and S. Routier, *Eur. J. Org. Chem.*, 2012, 3079.

30 E. Krieger, B. S. Nabuurs and G. Vriend, *Homology modeling*, 2003, **44**, 509.

31 J. Lecka, G. Ben-David, L. Simhaev, S. Eliahu, J. Oscar Jr, P. Luyindula, J. Pelletier, B. Fischer, H. Senderowitz and J. Sévigny, *J. Med. Chem.*, 2013, **56**(21), 8308.

32 S. Jansen, A. Perrakis, C. Ulens, C. Winkler, M. Andries, R. P. Joosten, M. Van Acker, F. P. Luyten, W. H. Moolenaar and M. Bollen, *Structure*, 2012, **20**, 1948.

33 *Molecular Operating Environment (MOE)*, 2013.08, Chemical Computing Group Inc, 1010 Sherbooke St. West, Suite #910, Montreal, QC, Canada, H3A 2R7, 2016.

34 R. A. Laskowski, M. W. MacArthur, D. S. Moss and J. M. Thornton, *J. Appl. Crystallogr.*, 1993, **26**(2), 283.

35 S. I. Belli and J. W. Goding, *Eur. J. Biochem.*, 1994, **226**, 433.

36 P. Jinhua, J. W. Goding, H. Nakamura and K. Sano, *Genomics*, 1997, **45**, 412.

37 E. Kaczmarek, K. Koziak, J. Sévigny, J. B. Siegel, J. Anrather, A. R. Beaudoin, F. H. Bach and S. C. Robson, *J. Biol. Chem.*, 1996, **271**, 33116.

38 S. M. Vlajkovic, G. D. Housley, D. Greenwood and P. R. Thorne, *Mol. Brain Res.*, 1999, **73**, 85.

39 A. F. Knowles and W. C. Chiang, *Arch. Biochem. Biophys.*, 2003, **418**, 217.

40 T. M. Smith and T. L. Kirley, *Biochim. Biophys. Acta*, 1998, **1386**, 65.

41 F. Kukulski, S. A. Lévesque, E. G. Lavoie, J. Lecka, F. Bigonnesse, A. F. Knowles, S. C. Robson, T. L. Kirley and J. Sévigny, *Purinergic Signalling*, 2005, **1**, 193.

42 M. M. Bradford, *Anal. Biochem.*, 1976, **72**, 248.

43 M. Ashraf, S. M. A. Shah, I. Ahmad, S. Ahmad, S. Arshad, K. Ahmad and F. H. Nasim, *J. Med. Plants Res.*, 2011, **5**(10), 2090.

44 A. Tashfeen, H. Shahid, A. A. M. Najim, L. Roberta and L. Paolo, *Acta Pharm.*, 2008, **58**, 135.

45 J. Wang, R. M. Wolf, J. W. Caldwell, P. A. Kollman and D. A. Case, *J. Comput. Chem.*, 2004, **25**, 1157.

46 R. Hoffmann, *J. Chem. Phys.*, 1963, **39**, 1397.

47 N. M. O'Boyle, M. Banck, C. A. James, C. Morley, T. Vandermeersch and G. R. Hutchison, *J. Cheminf.*, 2011, **3**(1), 1.

48 *Discovery StudioVisualizer 4.0*, Accelrys Software Inc, 2005.